

**SELF REPORT**

*ZnO quantum wells in Zn(Mg,Cd)O nanocolumns and planar structures, grown on selected substrates*

**Mieczysław A. Pietrzyk**



**PAS Institute of Physics**

<b>1. Name and surname.....</b>	<b>3</b>
<b>2. Education and academic degrees .....</b>	<b>3</b>
<b>3. Information about employment .....</b>	<b>3</b>
<b>4. Description of the achievements, set out in art. 219 para 1 point 2 of the Act .....</b>	<b>3</b>
4.1. Title of the scientific achievement.....	3
4.2. List of publications constituting the scientific achievement.....	3
4.3. Description of the achievements.....	4
4.4. Bibliography .....	27
<b>5. Information on scientific activity .....</b>	<b>28</b>
5.1. Description of scientific output not related to the habilitation thesis before obtaining a Ph. D. degree in physics .....	28
5.2. Description of scientific achievements not related to the topic of habilitation, after obtaining the PhD .....	30
5.3. Information on presentations at national or international scientific or artistic conferences, detailing the invited lectures and plenary lectures.....	32
5.4. Information on participation in the organizational and scientific committees of national or international conferences, including the function performed.....	34
5.5. Information on participation in the work of research teams implementing projects financed through domestic or foreign competitions/grants, with a division into completed and ongoing projects, and including information on the function performed within the team's work. ....	34
5.6. Information on internships in scientific or artistic institutions, including foreign ones, including the place, date, duration, and nature of the internship .....	35
5.7. Information on peer-reviewed scientific or artistic papers, in particular those published in international journals .....	35
5.8. Obtained industrial property rights, including obtained patents, national or international .....	35
5.9. Information on expert opinions or other studies commissioned by public institutions or entrepreneurs.....	36
<b>6. Information about the achievements in teaching, organization and popularizing science or art .....</b>	<b>36</b>
<b>7. In addition to the issues listed in point 1-6, the applicant may provide other information, important from his point of view, regarding his professional career.....</b>	<b>36</b>

## 1. Name and surname

Mieczysław Antoni Pietrzyk

## 2. Education and academic degrees

- 2005-2010    Polish Academy of Sciences, Institute of Physics in Warsaw  
Scientific degree: PhD in physics  
Dissertation title: *Wkład otwartych powłok 3d i 4f do struktury elektronowej wybranych półprzewodników IV-VI z Mn, Gd i Eu.*  
Thesis supervisor: prof. dr hab. Bogdan Kowalski
- 1999-2004    Silesian University of Technology in Gliwice  
Scientific degree: MSc engineer  
Master's thesis: *Elektryczne i akustyczne badanie dwuwarstwowych struktur sensorowych*  
Thesis supervisor: 

prof. dr hab. Marian Urbańczyk
--------------------------------

## 3. Information about employment

- 01.04.2018 to present    PAS Institute of Physics  
*Assistant Professor*
- 01.01.2010-31.03.2018    PAS Institute of Physics  
*Physicist*
- 01.01.2005 – 31.12.2009    PAS Institute of Physics  
*PhD student*

## 4. Description of the achievements, set out in art. 219 para 1 point 2 of the Act

### 4.1 Title of the scientific achievement

**ZnO quantum wells in Zn(Mg, Cd)O nanocolumns and planar structures, grown on selected substrates**

### 4.2 List of publications constituting the scientific achievement

[H1] M.A. Pietrzyk, M. Stachowicz, A. Wierzbicka, P. Dłuzewski, D. Jarosz, E. Przedziecka A. Kozanecki, *Growth conditions and structural properties of ZnMgO nanocolumns on Si(111)*, J. Cryst. Growth 408 (2014) 102-106

[H2] M.A. Pietrzyk, M. Stachowicz, A. Reszka, A. Kozanecki, *Optical investigations of ZnO/ZnMgO quantum wells in self-assembled ZnMgO nanocolumns grown on Si (111) by MBE*, J. Lumin. 179 (2016) 610-615

- [H3] M.A. Pietrzyk, M. Stachowicz, D. Jarosz, R. Minikayev, M. Zielinski, P. Dluzewski, A. Kozanecki, *Properties of ZnO/ZnMgO nanostructures grown on r-plane Al<sub>2</sub>O<sub>3</sub> substrates by molecular beam epitaxy*, J. Alloys Compd. 650 256-261 (2015)
- [H4] M.A. Pietrzyk, M. Stachowicz, A. Wierzbicka, A. Reszka, E. Przeddziecka, A. Kozanecki, *Properties of ZnO single quantum wells in ZnMgO nanocolumns grown on Si (111)*, Opt. Mater. 42 406–410 (2015)
- [H5] M. A. Pietrzyk, M. Stachowicz, P. Dluzewski, A. Wierzbicka, A. Kozanecki, *Self-organized ZnMgO nanocolumns with ZnO/ZnMgO quantum wells on c-plane Al<sub>2</sub>O<sub>3</sub> substrates by MBE: growth conditions and properties*, J. Alloys Compd. 737, 748-751 (2018)
- [H6] M.A. Pietrzyk, A. Wierzbicka, M. Stachowicz, D. Jarosz, A. Kozanecki, *Fabrication and characterization of ZnMgO nanowalls on 4H-SiC by MBE method*, J. Appl. Crystallogr. 52, 168-170 (2019)
- [H7] M.A. Pietrzyk, A. Wierzbicka, E. Zielony, A. Pieniazek, R. Szymon, E. Placzek-Popko, *Fundamental studies of ZnO nanowires with ZnCdO/ZnO multiple quantum wells grown for tunable light emitters*, Sensor. Actuator. A- Phys. 315, 112305 (2020)
- [H8] M.A. Pietrzyk, E. Placzek-Popko, K.M. Paradowska, E. Zielony, M. Stachowicz, A. Reszka, A. Kozanecki, *Optoelectronic properties of ZnO/ZnMgO multiple quantum wells in ZnMgO nanocolumns grown on Si (111)*, J. Alloys Compd. 717, 41-47 (2017)
- [H9] M. Stachowicz, M.A. Pietrzyk, J.M. Sajkowski, E. Przeddziecka, H. Teisseyre, B. Witkowski, E. Alves, A. Kozanecki, *Asymmetric ZnO/ZnMgO double quantum well structures grown on m-plane ZnO substrates by MBE*, J. Lumin. 186, 262-267 (2017)
- [H10] J. Andrzejewski, M. A. Pietrzyk, D. Jarosz, A. Kozanecki, *Optical measurements and theoretical modelling of excitons in double ZnO/ZnMgO quantum wells in an internal electric field*, Materials, 14, 7222 (2021)

### 4.3 Description of the achievements

#### Introduction – the scientific background of the research

In the last decade, there has been a growing interest in research of wide bandgap semiconductors. Among such materials, zinc oxide (ZnO) has received special attention due to its unique and very promising properties: high electron mobility, high thermal conductivity, very high exciton binding energy 60 meV in room temperature (GaN = 25 meV) – these are properties that make ZnO an attractive material for applications in optoelectronics, piezoelectric devices, transparent electronics, spin electronics and chemical sensors [2, 3]. Apart from its wide bandgap (3.3 eV) [4], the ZnO are characterized by its high optical transmission in visible spectrum, as well as by easily controllable electrical parameters (a wide range of electron concentrations and mobility) depending on the deposition conditions [5]. ZnO is a widely available material that is also bio-compatible, non-toxic and safe for living beings, that is why it is used in medicine, cosmetics or stomatology. Due to its high applicability, ZnO has become the most studied (after Si and GaN) semiconductor within a decade.

One of the interesting and undoubtedly applicational properties of this material is the possibility of changing its bandgap width using Mg or Cd doping. It allows for manufacturing of ternary materials like ZnMgO or ZnCdO, with higher or lower bandgap energy, which are essential for fabrication of quantum wells and laser structures. The structures with ZnO/Zn(Mg,Cd)O quantum wells enable to increase the luminescence intensity, and this is not only very significant for application in efficient light sources, but also interesting considering their use in transparent electronics.

The ternary ZnCdO compound can cover a spectral range extending it from the ultraviolet to blue and even green light which is essential to construct appropriate light emitting diodes based on ZnCdO-related heterostructures or quantum wells [6].

Introduction of Mg or Cd into the ZnO crystal not only affects the bandgap energy but also the parameters of crystal lattice, which change with the increasing amount of the dopant.

ZnMgO has a great advantage over other materials, as its lattice mismatch with ZnO is only 1%. This fact, and large „band offset” (about 1 eV) [7] allow for successful production of ZnMgO/ZnO/ZnMgO nanostructures.

In my work, I focused on application of Mg and Cd in ZnO. In my experiments and studies included in this habilitation thesis, I modified the bandgap by changing the concentration of the dopants, which allowed for studying of quantum wells, multiple quantum wells and superlattices, their characterization and examination of luminescent recombination processes, to obtain a stable and efficient blue and green luminescence. In the ZnO/Zn(Mg,Cd)O quantum structures, exciton binding energy can increase up to 100 meV, making the emission efficient in temperatures over 300K. The cathodoluminescence measurements, performed in room temperature and presented in the works from the habilitation thesis, are a good example.

The one-dimensional (1D) Zn(Mg,Cd)O nanostructures such as nanotubes, nanowires, nanorods, and nanoribbons [eg. 8,9] stimulate considerable interests for scientific research due to their importance in fundamental physics studies and their potential applications in nanoelectronics, nanomechanics, and flat panel displays. Particularly, the optoelectronic device application of 1D Zn(Mg,Cd)O nanostructures becomes one of the major focuses in recent nanoscience researches. An important issue in self-organizing growth of 1D nanostructures in a way of controlling of their morphology, position, orientation, and crystallographic quality. These particular problems became the subject of my scientific interest after completing my PhD degree.

The price of semiconductor devices depends greatly on the size and quality of the crystalline substrate on which the device structure is epitaxially deposited, that is why the choice of the substrates I used for my studies was carefully planned.

The most common orientation of crystal growth for oxide is in a polar direction  $c$  (0001). This is the case of growth on silicon and sapphire substrates  $a$  (11-20) and  $c$  (0001) crystallographic direction. This is the case of growth on silicon and sapphire substrates  $a$  (11-20) and  $c$  (0001) crystallographic direction.

Very interesting is the growth on  $c$  -plane (0001) sapphire substrate. In this direction, a strong built-in electric field is present due to spontaneous and piezoelectric polarization.

For ZnO/ZnMgO quantum wells (QWs), the spontaneous and piezoelectric polarization on both sides of the well is a source of built-in electric charge of opposite sign. The existence of this internal electric field generates a linear potential and as a result, lowers the energy of quantum states in the well, and for the wide wells, the electrons are spatially separated from the holes.

One of the consequences of the presence of such fields is a quantum confined Stark effect (QCSE), resulting in spatial separation of electron and hole wave functions in quantum wells, and lowering the possibilities of radiative transitions – a very inconvenient effect for optoelectronic applications. The energy levels bend, and the triangular quantum well is created, and the emission energy from such well can be lower than the bandgap in bulk material.

The internal electric field can be screened by high density of free carriers – such effect can be achieved by injecting the carriers into the sample (electroluminescence) or generating them by optical pumping (photoluminescence). That kind of screening leads to minimization of Stark effect and shifting the spectra towards shorter wavelengths. The screening problem is well analyzed and described for nitrides [10-13] but for oxides the reports are scarce. For example, in the studied InGaN/GaN wells the piezoelectric-induced Stark effect dominates for well widths above 3 nm and with low In content (lower than 15-20 %) [14].

To avoid the “activity” of electric fields, the piezoelectric polarization must be minimized by applying a lattice-adjusted wells and barriers. It can be achieved by optimization of growth processes of ZnO/ZnMgO structures. Matching of crystal lattice of wells and barriers allows to avoid strains (causing cracking and/or creating dislocations in material).

Since, as it was mentioned before, the structures will be manufactured on different substrates with different lattice constants and different orientations, we have also studied the strain relaxation depending on Mg amount and the type of the structure (nanowires, nanocolumns). Tensions and strains present in material can lead to change of physical properties of the examined structures.

The presented habilitation thesis covers both the fundamental research of optical and structural properties of quantum structures in nanocolumns and planary layers, and the elaboration of growth procedures.

Hence, the dissertation was divided into two parts: the first part presents the growth parameters for planary structures and nanocolumns grown on different substrates, and their structural properties. In the second part I present the results of optical studies of quantum wells located in these nanostructures. Structural measurements were performed using the scanning electron microscope (SEM), X-ray diffraction (XRD) and atomic force microscope (AFM). Transmission electron microscopy (TEM) confirmed the presence of ZnO quantum wells, their interactions, and precisely determined the width of the obtained wells.

The most important were the optical measurements. Luminescence measurements (photo- and cathodoluminescence) in various temperatures provided information on the emission properties of manufactured structures.

## **Research results**

In order to study and describe quantum phenomena, and at the same time to fully use the application potential of ZnO-based nanostructures in opto- and micro-electronics, it is necessary to obtain good quality structures both in terms of structure and optics.

One of the objectives of my work was elaborating the growth parameters for ZnMg(Cd)O planar structures and nanocolumns on various substrates, with different lattice constants, orientations and polarities, manufactured with MBE technique. It is worth to mention, that when I began working on this issue, there was almost no available reports on spontaneous ZnO growth, without a catalyst. At the moment, such reports are still very scarce. This problem is noticed and described by Sallet *et al.* [11].

The elaboration of procedures for columnar growth is of great application importance. The surface to volume ratio in nanowires is very high, which makes them ideal to use as sensors, photodetectors or light emitters. The shape of nanowires makes it also much easier to relax the strain generated by the lattice mismatch between the structures and the substrate, and as a result – to avoid creation of defects.

The process of nanocolumn formation without a catalyst proceeds spontaneously, and is induced only by strains caused by lattice mismatch between the substrate material and the nanocolumn material. The advantage of such method is that the nanocolumns are created spontaneously, without applying any other procedures such as lithography or implantation. This type of growth makes it possible to obtain innovative ZnO/Zn(Mg,Cd)O structures in one technological process. A disadvantage of this process is lack of control over the location of nanocolumns and the fact that they grow in different sizes. The reports mentioned below show, that obtaining of planar or columnar structure depends greatly on the initial growth parameters, buffer layer growth temperature, structure growth temperature, and the oxygen to zinc ratio [H1-H4]. One should keep in mind that, of course, for every kind of substrate one must adjust a different growth parameters. The choice and preparation of the surface affects the concentration of defects and strains, and as a consequence, the optical and structural properties.

Having developed the procedure for growing nanostructures, and knowing their structural properties, the next step was examining the optical properties of quantum structures (single and multiple quantum wells and super-lattices) located in these nanostructures.

Most of the works presented in this habilitation thesis was published within the SONATA project, founded by NCN (National Science Centre) entitled: "ZnO quantum wells in ZnMgO nanocolumns grown on selected substrates with MBE technique", for which I was the Principal Investigator.

### **Mechanisms of ZnO / ZnMgO nanocolumn growth on a silicon substrate with crystallographic direction (111)**

As the first step, we have elaborated the growth procedure for ZnMgO nanocolumns on Si surfaces. Growing such structures on silicon is difficult due to a substantial lattice mismatch (40%) and a fast oxidation of the substrate, but it is very important since Si plays a crucial role for development of opto- and nanoelectronics.

In [H1] the nanocolumn growth with and without a ZnO buffer layer was discussed. It was most likely the first publication ever presenting the nanocolumn growth without a catalyst. The growth process without a buffer layer was performed in temperature 550°C, in oxygen-rich conditions. The diameter of obtained nanocolumns was about 30 nm. For the other process, a 400 nm ZnO buffer layer was grown at 450°C, while the columnar structures were grown at 840°C. Diameter of the nanocolumns obtained this way was about 50 nm. Increasing the temperature of buffer layer growth to 550°C (and subsequently growing nanocolumns in the same conditions as before) caused the diameter of nanocolumns change to about 35 nm. We can clearly see that the temperature of buffer layer growth influences the size of the nanocolumns.

The TEM measurements have shown that during the growth process, a thin (3-4 nm) SiO<sub>2</sub> layer is created, and the nanocolumns grow directly on this layer [H1]. It is caused by the strong oxidation of silicon substrates. We can observe a similar situation while growing GaN

on Si, when a thin layer of  $\text{Si}_x\text{N}_y$  is created [12]. XRD measurements show that structures grown on Si are hexagonal, and grow always in  $c$  direction.

In experiments presented in [H2], the growth temperatures were a bit modified: ZnO buffer layer was grown at  $450^\circ\text{C}$ , while the nanocolumns with ZnO/ZnMgO quantum structures were grown at a very high temperature, at  $940^\circ\text{C}$ . It allowed for obtaining the nanocolumns with diameter of about 30 nm.

Apart from eliminating the differences between the substrate and e.g. quantum structure, low temperature buffer layer improves the adhesion of epitaxial Zn(Mg)O layer to the Si surface, preventing the epitaxial layer „peeling away” from the substrate. Therefore, as it was presented above, the right choice of the temperature of the buffer layer growth is of great importance, as it has a significant effect on the size of nanocolumns.

### Mechanisms of ZnO/ZnMgO nanocolumn and planar structures growth on $r$ -plane semi-polar sapphire substrates

The next work in habilitation thesis pertains to the growth process on  $r$ -plane semi-polar sapphire substrate [H3]. This type of substrate is very important for optical studies, since, as we will see later, the MgZnO structure grows on this substrate in non-polar  $a$  direction. It was possible to tune the growth parameters to obtain whether the columnar (Fig.1a) or planar (Fig.1b) growth. To obtain the planar growth we used a low temperature ZnO buffer layer, and then deposited the relevant ZnMgO layer in higher temperature ( $550^\circ\text{C}$ ). If the buffer layer is not applied, such a growth procedure in oxygen-rich conditions will result in formation of nanocolumns tilted  $62^\circ$  to the surface. X-ray measurements indicated, that on  $r$ -plane sapphire the planar structure grows in non-polar  $a$  direction, while the nanocolumnar structure two growth directions, a nad  $c$ , were observed. It is caused by the fact that, to obtain nanocolumns, the thin layer (about 10 nm) of ZnO was first deposited in Zn-rich conditions, and then the conditions were quickly switched to oxygen-rich to obtain nanocolumnar growth. The thin layer of ZnO grows in  $a$  direction, while the nanocolumns grow in polar  $c$  direction. No other phases of ZnO and ZnMgO were observed [H3]. Our results are in line with the results presented by Aschenbrenner *et al.* [17] for nitrides. This group describe self-organized growth of GaN nanorods without catalyst on  $r$ -plane sapphire using a combination of molecular beam epitaxy and metal–organic vapor-phase epitaxy. They observed that nanorods are inclined by  $62^\circ$  towards the  $\pm[1100]$ -directions. We obtained probably first inclined ZnMgO nanocolumns growth on  $r$ -plane  $\text{Al}_2\text{O}_3$  by MBE method in one technological process.

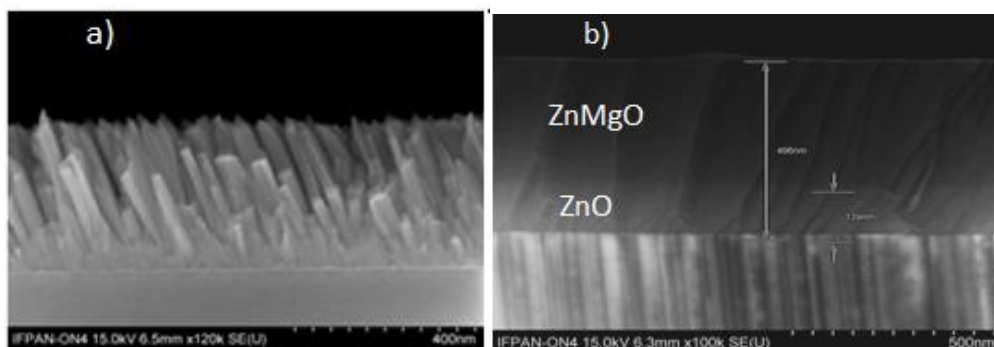


Fig. 1. ZnMgO nanostructures on  $r$ -plane sapphire substrate a) without a buffer layer b) with a low-temperature ZnO buffer layer [H3]

## **Influence of growth conditions on properties of ZnO/ZnMgO nanocolumns grown on *c*-plane polar sapphire substrates**

In [H5] the growth on the commercial *c*-plane polar sapphire substrate is presented. Unlike the nitride structures, *c*-plane sapphire is seldom used for growing of ZnO/ZnMgO structures, usually because of the large lattice mismatch (about 15%). As it was mentioned before, there are strong internal electric fields present in this direction. My expertise with growing structures on Si allowed me to master the technology of nanocolumn growth also on this type of substrate.

My original idea was to use a 3 x ZnO + 2 x MgO buffer seen in the TEM image (Fig. 2.) on a polar *c*-oriented sapphire substrate. Thus, the columnar growth was achieved. The obtained nanocolumns have diameter about 30 nm, and were grown in 550°C in oxygen-rich conditions [H5]. Application of MgO buffer leads to the creation of ZnMgO monolithic layer, as reported in [18, 19].

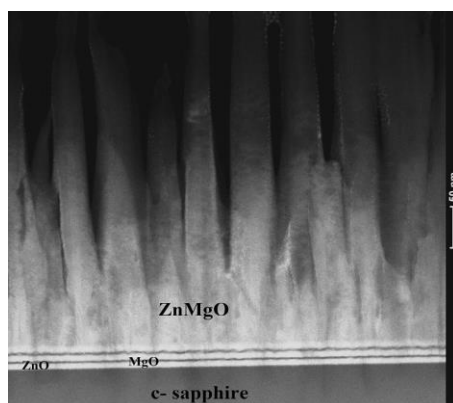


Fig.2 Columnar growth of ZnMgO on a *c*-plane sapphire substrate with application of 3 x ZnO + 2 x MgO buffer layer [H5].

## **Investigation of the influence of 4H-SiC substrate on the growth of ZnO/ZnMgO nanostructures**

Silicon carbide (SiC) is a semiconductor material with large bandgap (up to 3.26 eV), characterized by a high thermal conductivity, high breakdown voltage and high switching frequency, which make it an attractive candidate to use in high power and frequency applications [20, 21]. SiC is also known for its excellent mechanical properties and good chemical stability [22,23]. Most of these qualities results from its crystal structure, and presence of various polymorphs (most widely known are 3C-SiC, 4H-SiC i 6H-SiC). A good lattice matching between ZnO and SiC enable to fabricate nanostructures with excellent electric and optical qualities. Despite the interesting properties of this material, the growth of ZnMgO nanocolumns on SiC was not well described in scientific literature. One of the main limitations is a very high price of high quality SiC crystals. In my experiments I used the 4H-SiC polymorph, and the growth was performed on Si side, without any Au or Ag catalyst.

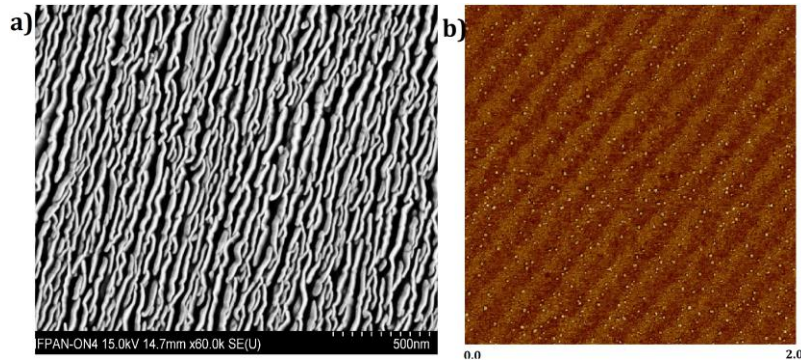


Fig. 3. a) SEM image of ZnMgO surface grown on 4H-SiC substrate b) AFM image of clean 4H-SiC substrate

A SEM image of the ZnMgO/4H-SiC surface reveals that the structure consists of nanowalls (Fig. 3a) regularly arranged in parallel rows [H6]. The nanowall height is about 460 nm (as estimated from the growth conditions) and their thickness is about 15-20 nm. The nanowalls are perpendicular to the surface of the 4H-SiC substrate. Fig. 3b shows an atomic force microscopy (AFM) image of the SiC substrate used for growth. The clean SiC surface consists of nanostripes, parallel to each other. The nanowalls are oriented along these stripes. We can therefore conclude that the type of substrate defines the shape of obtained nanostructures. The growth process was performed in 550°C in oxygen-rich conditions, without a buffer layer, directly on the clean 4H-SiC surface. The crystal quality was studied with HR-XRD and is thoroughly described in [H6].

### **Investigation of ZnO / ZnCdO quantum nanostructures produced on silicon substrates at a very low deposition temperature**

An interesting issue was obtaining ZnO/ZnCdO quantum structures on silicon substrates with ZnO buffer layer. In this case the growth temperature had to be low (170°C) to avoid Cd desorption from the surface due to its volatility. In [H7] we present the structural and luminescence properties of ZnO nanowires with 30 period multiple ZnCdO/ZnO quantum wells (QWs and barriers widths were about 2 nm), grown without a catalyst directly on Si(111) surface. Nanowire diameters are about 40-45 nm.

The XRD measurements shows that the structures are hexagonal and polar. The analysis of the XRD data yielded the SL mean period equals to  $(52.5 \pm 0.1) \text{ \AA}$ . From  $2\theta/\omega$  scans the averaged c lattice parameter of SL is  $c_{SL} = 5.2115 \text{ \AA}$ . The mean period calculated from XRD measurements equals to  $(40 \pm 10) \text{ \AA}$ . Moreover, the XRD experiments show a broadening of XRD signal on RSMs. It can be due to micro-strain generated in nanowires structure caused by coalescence of nanowires. Coalescence of nanowires is visible on the SEM image.

The micro-Raman spectra obtained with 514.5 nm excitation wavelength show phonon modes originating from the Si substrate as well as the ZnO layer of ZnCdO/ZnO heterostructures. The positions of particular phonon modes are shifted towards lower frequencies at about  $2\text{-}3 \text{ cm}^{-1}$  with respect to the positions of the same phonon modes in Raman spectrum of bulk ZnO. A red-shift of the ZnO-like phonon modes may indicate a tensile type of strain in the ZnCdO/ZnO sample, which can be caused by the presence of Cd in ZnCdO alloy of ZnCdO/ZnO MQWs or it may be due to coalescence of nanowires as well.

## Optical properties of nanocolumns with ZnO/ZnMgO quantum wells

Apart from developing a technology of ZnMgO nanowire growth, simultaneously we performed the studies of single and multiple quantum structures with various widths, located in these nanostructures. An attempt was made to describe the recombination process mechanism in dependence of QW width and of the distance between the QWs in single nanocolumns (so-called coupled quantum wells). The quantum-confined Stark effect was also studied, in double asymmetric quantum wells for the substrates on which the ZnO/ZnMgO structures were growing in polar direction.

### Optical analysis of ZnMgO nanocolumns and ZnO/ZnMgO quantum wells located in these nanocolumns, grown on a Si (111) substrate

Apart from the growth conditions for ZnMgO nanowires on Si described above, [H1] presents also results of the optical measurements for ZnMgO nanostructures without quantum wells. Optical analysis was performed using photo- (PL) and cathodoluminescence (CL). PL spectra were measured in temperature range 11.5–300 K, while the CL spectra are measured at room temperature. Both spectra confirm (it is especially clearly visible in CL spectrum) the emission from ZnMgO structure at 3.52 eV, while the broad signal at 3.385 eV can be attributed to the emission from excitons bound to the neutral donor ( $D^0X$ ).

With increasing measurement temperature, the  $D^0X$  peak is gradually shifting to lower energy, from 3.520 eV at 11.5 K to about 3.344 eV at 300 K. The emission associated with free excitons (FX) appears as a shoulder at the higher energy side of the  $D^0X$  peak. This emission line is located at about 3.4 eV at 11.5 K. The FX emission takes over after 50 K, becoming dominant with a further temperature increase. This interaction between  $D^0X$  and FX excitons is typical for oxide structures. We observed optical phonon (LO) replicas of recombination of excitons bound to neutral donors 1LO at 3.314 eV, 2LO at 3.240 eV and 3LO at 3.168 eV.

The next step of our studies was the optical characterization of single ZnO/ZnMgO quantum wells with various widths, localized in ZnMgO nanowires grown on silicon substrate [H4]. The right choice of growth parameters is crucial in this case, especially the Zn/Mg ratio, because if the Mg content is too low, it can be insufficient for obtaining a relevant barrier.

We have studied the positions of the PL lines from QWs depending on the well width for the same ZnMgO barrier height. In Fig. 4a, the PL spectra measured at 10K for three ZnMgO/ZnO/ZnMgO QW structures with the well widths of 2 nm, 2.5 nm and 3 nm, are presented. We observed a redshift of excitonic emission from the wells in comparison to bulk ZnO. One must keep in mind that high exciton binding energy (60 meV) is directly linked to the small Bohr radius  $a_B$  of about 1.8-2.0 nm. FWHM of the PL peaks increases with the decreasing well layer thickness and this is due to the increasing contribution of nonuniformities in composition at the interfaces into the PL emission. Our results agree well with the results by He *et al.* [24]

Figure 4b shows the monochromatic cathodoluminescence map from the cross-section and the SEM image of the cross-section of the structure. On the map, we can observe a distinct emission at 3.31 eV coming from a single quantum well. Thus, the CL mapping results confirm the existence of single quantum wells in nanocolumns. The ability to distinguish the emissions from the 2, 2.5 and 3 nm wells confirms the very good quality of our structures.

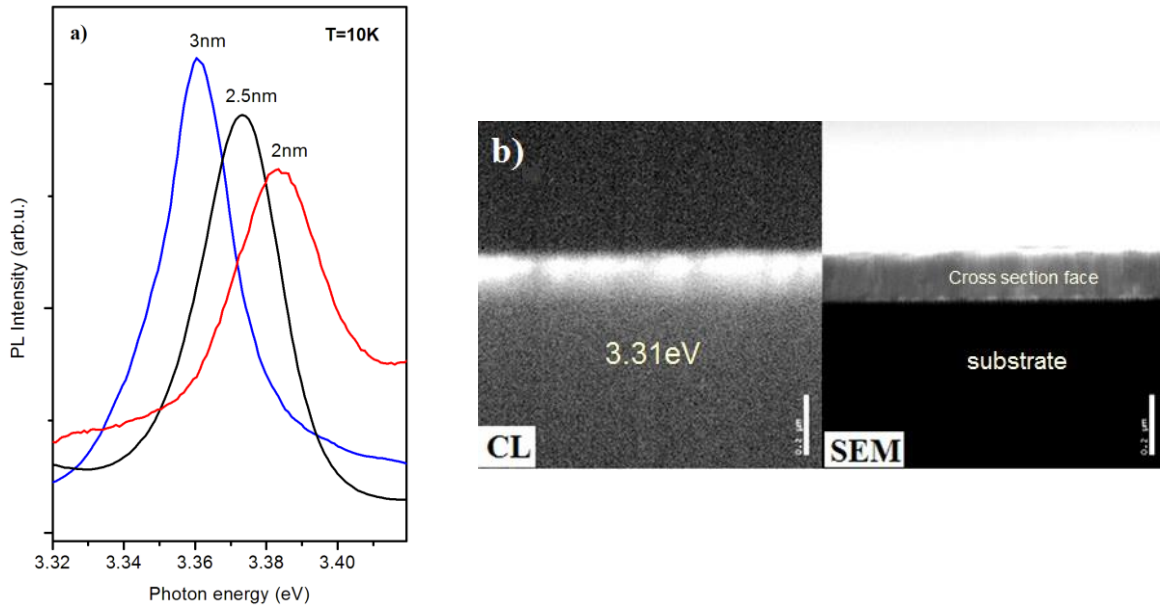


Fig. 4 a) PL spectrum for single quantum wells of different widths b) CL map and cross-section of the structure [H4]

Another stage of our research is the fabrication and study of double asymmetrical ZnO QWs in nanocolumns, separated by ZnMgO barriers of two different widths (100 nm and 3 nm), grown in high temperature (940°C) without a catalyst. The intention of this experiment was to observe a coupling between two asymmetric QWs. The structure with 100 nm barrier was taken as a reference structure. The results are described in detail in [H2].

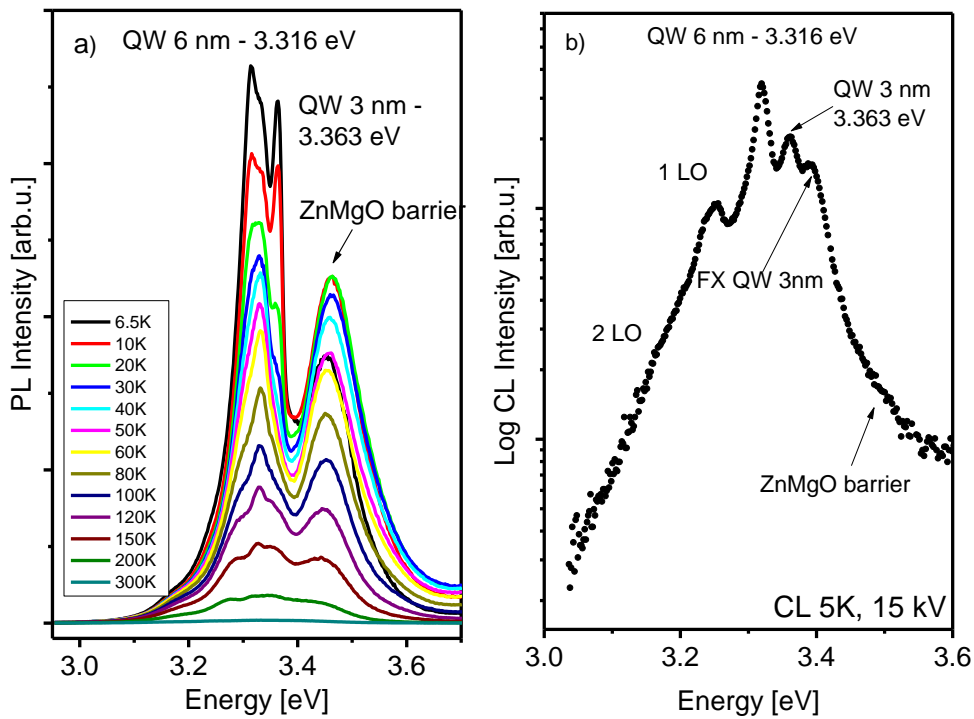


Fig. 5 a) Temperature dependence of photoluminescence and b) CL spectrum in 5K for the ZnO/ZnMgO structure with a 100 nm barrier [H2]

Fig. 5a shows photoluminescence spectra of the structure with quantum wells (3 and 6 nm) separated by a 100 nm ZnMgO barrier. These PL spectra exhibit three main emission lines. The emission line observed at 3.363 eV we assigned to a 3 nm and at 3.316 eV line to a 6 nm QW. The 3.47 eV emission peak originates from excitonic recombination in ZnMgO barrier. Based on the PL spectrum the content of Mg has been estimated to approximately 12%. However, another peak appeared at 3.333 eV, which we believe is the PL from the excitonic recombination ( $1e \rightarrow 1hh$ ) - first electron level in the conductive band to first heavy hole level in the valence band in the 6 nm QW. Its intensity decreases slowly with increasing temperature, being still distinguishable at RT. This fact, together with the results of theoretical calculations, are the facts supporting this thesis. The calculations were performed using EPITAXY project software [25] for the electron effective mass  $m_e^* = 0.28 m_0$  [27] and the hole effective mass  $m_h^* = 0.59 m_0$  [27]. The obtained value of  $3.334 \pm 0.0171$  eV agrees well with the experimental one indicating excitonic transition from first electron to first light hole level. We obtained a very similar spectrum by CL measurements at 5 K. The positions of the peaks from quantum wells are at the same photon energies as in the PL spectrum (Fig. 5 b). Other CL lines at 3.249 eV and 3.162 eV we assign to 1 LO and 2 LO replicas respectively.

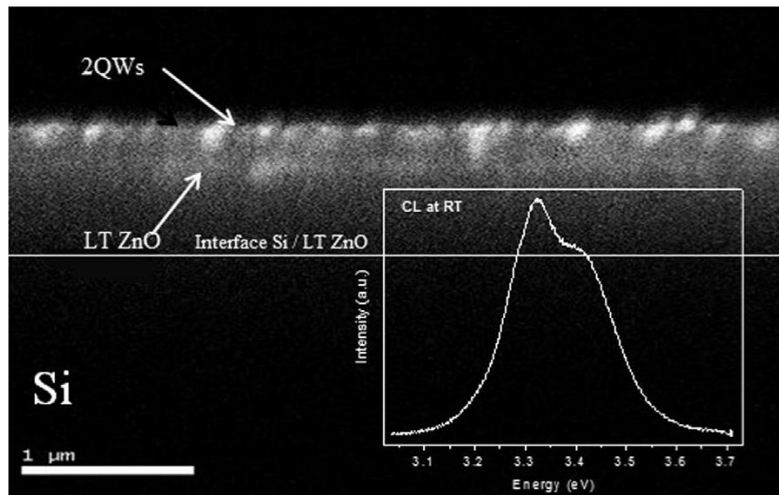


Fig. 6. Monochromatic CL image of the cross-section of a sample with a double quantum well with a ZnO buffer layer, measured at room temperature (insert - CL spectrum at 15 kV) [H2].

In Fig. 6 the cross-sectional SEM-CL image is presented. The room temperature cross-sectional monochromatic CL mapping of the sample clearly shows two light areas. We can see the emission from two ZnO QWs of 6 and 3 nm in the upper part on the sample and LT ZnO. In the insert the CL spectrum measured at RT is also shown. Two broad peaks are observed: at around 3.416 eV originating from the ZnMgO barrier/capping and at 3.325 eV is contributed to confined excitons in the ZnO wells.

Fig. 7a presents a monochromatic CL map of the structure with two quantum wells (3 and 6 nm) separated by 3 nm ZnMgO barrier between the wells taken at room temperature, which reveals localized exciton recombination from both QWs in the upper part of the image an LT ZnO buffer.

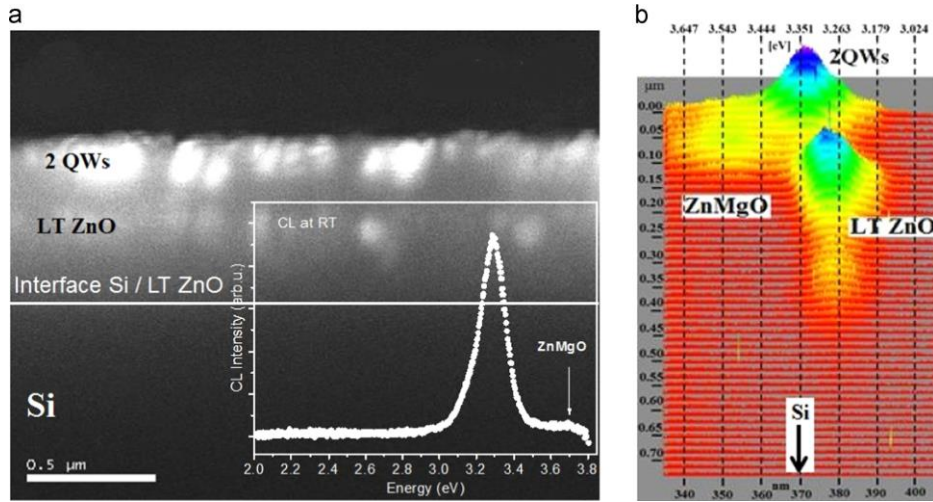


Fig. 7. Cathodoluminescence measurements at room temperature: a) CL map and CL spectrum from the surface (insert), applied acceleration voltage AV = 15 kV b) cross-sectional line scan of CL spectra, AV = 5 kV [H2].

A CL spectrum excited with electron beam normal to the surface at the acceleration voltage (AV) of 15 kV is shown in the insert. The CL spectrum reveals two peaks at 3.293 eV (QWs) and 3.73 eV (ZnMgO barrier). The observation of separate emissions from individual QWs at room temperature is not possible because the distance between them is too small (3 nm), and due to temperature broadening of the emission. Going towards the Si substrate, the CL from QW decreases gradually. Right below the emission from the ADQW's structure, one can see the emission near the interface between the ZnMgO barrier layer and LT ZnO buffer layer. The large lattice mismatch between Si substrate and LT ZnO buffer layer is a source of defects, which is the main reason why we do not see emission from a lower part of the ZnO region.

Fig. 7b shows the cross-sectional CL spectrum line scans of the ZnMgO/ZnO structure along the  $c$ -axis at 5K temperature. The acceleration voltage of the electron beam was 5 kV. The CL scan direction was from the surface towards the substrate. The image is composed of 47 spectra and represented as a two-dimensional plot, where the intensity is color coded. The LT ZnO buffer, two ZnO/ZnMgO QWs and the ZnMgO barrier emissions are labeled. It can be noticed that a relatively intense CL from the ZnO buffer is observed in the distance more than 200 nm above the substrate.

In Fig. 8, the CL spectra at 5K excited with different electron energies are shown. The 1 kV beam may probe the sample up to about 20 nm in depth from the surface. At this energy one can observe only a peak at about 3.267 eV. According to Wu *et al.* [28] a possible origin of this luminescence can be due to surface states or acceptor impurities or excitons bound to structural defects. A 2 kV electron beam (maximum generation rate of e-h pairs at 20-30 nm) allows to observe a peak at 3.331 eV originating predominantly from the excitonic recombination ( $1e \rightarrow 1hh$ ) first electron level in the conductive band to first heavy hole level in the valence band in the 6 nm quantum well. The electron beam at 5 keV probes the structure deeper (50-150 nm) shifting the emission maximum toward higher energies to 3.361 eV which correlates with excitonic recombination in 3nm QW. The electron beam with energies above 10 kV excite the emission in whole quantum structure and reaches deeper into low temperature buffer, that is why we see also the emission of LT ZnO buffer (3.305 eV). Another feature of the QW structure revealed by beams a high energy is a contribution from excitonic transitions originating from  $1e \rightarrow 1lh$  levels transition (3.335 eV) in 6 nm QW. That

locations reflect the PL peaks and it is difficult to resolve them most probably because of the overlap between them, (Zippel *et al.* [29]). The free exciton (FX) QW 3nm peak is located at 3.387 eV but with ZnMgO barrier at 3.75 eV.

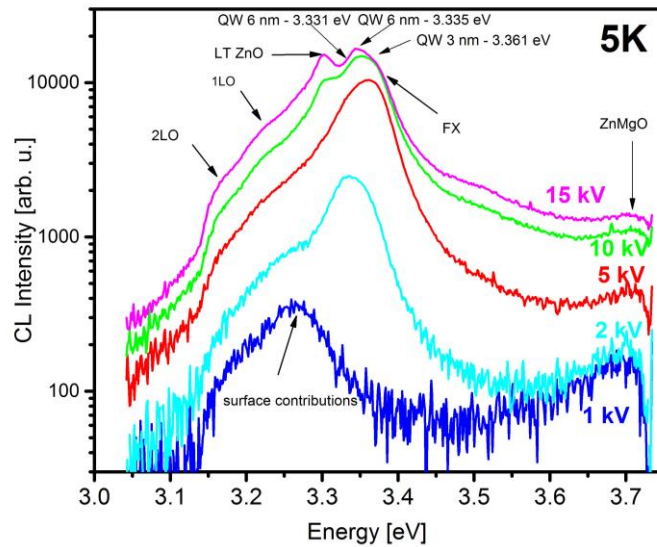


Fig. 8. CL spectra measured at 5K for various electron energies [H2]

The next important step was studying the ZnO/ZnMgO multiple quantum wells (MQWs) located in ZnMgO nanowires [H8]. For this purpose, the PL measurements of 10 period ZnO/ZnMgO quantum wells (3nm) with ZnMgO barrier (15 nm) were performed. The maximum observed at temperature 6K and energy about 3.381 eV corresponds to the MQW structure. In some of the higher energy spectra, a broad peak with maximum at about 3.60 eV is present. It is the emission from the ZnMgO barrier. The dominant emission in 150 K at 3.383 eV is most likely linked to the superposition of localized and free excitons in MQWs. Room temperature SEM-CL imaging was performed to confirm the origin of PL and the results are presented in Figure 9, which shows panchromatic and monochromatic SEM-CL imaging of the studied structure. Decomposition of the panchromatic image to monochromatic ones reveals a strong emission from the MQWs at 3.342 eV and from the ZnMgO barrier at 3.73 eV. The analysis of CL spectrum suggests, that in room temperature the emission from MQW exciton is dominant. The pictures clearly show a strong luminescence from single nanowires.

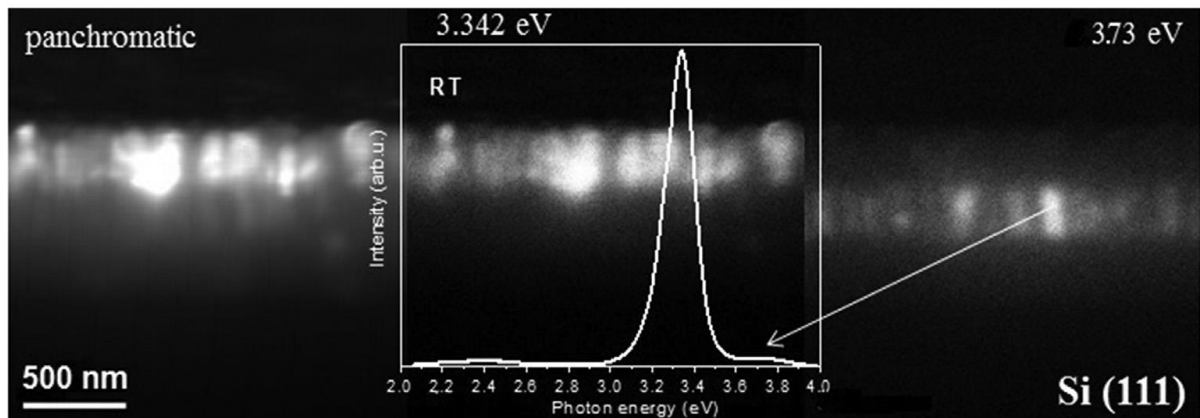


Fig. 9. Images of the CL cross-section of a 10-period MQW sample, measured at room temperature (insert - CL spectrum measured at 15 kV).

The luminescence spectra for wells with a narrower barrier were also analyzed. In nanocolumns localized ZnO/ZnMgO MQW structure containing 10 quantum wells each 1.7 nm wide with 2 nm ZnMgO inter-well barriers. The PL spectra shows weak emission observed at 3.725 eV comes from the ZnMgO cap/barrier layers. On this basis the Mg content has been estimated to be about 15%. The strong emission at 3.455 eV can be attributed to the recombination of the localized exciton in the ZnMgO/ZnO/ZnMgO MQWs. Two transitions denote 1LO and 2LO are longitudinal phonon (LO) replicas, since their position and energy distances match the 71 meV intervals counting from the position of MQWs. A weak peak at 3.363 eV at 8 K can be attributed to the emission of excitons bound to neutral donors ( $D^0X$ ) from the ZnO low temperature buffer.

Figure 10 shows cross-sectional CL-images of the 10-period MQW sample measured at room temperature. A panchromatic CL image (left side) can be decomposed to monochromatic images, and it is seen that indeed the emission at 3.65 eV comes from the ZnMgO buffer while emission at 3.42 eV corresponds to MQWs. Emission at 3.31 eV originates from two areas – close to ZnO/ZnMgO interface and from the surface where the MQW structure is located. It seems that this is emission is due to accidental coincidence of two different transitions related to the interface and surface states of the structure.

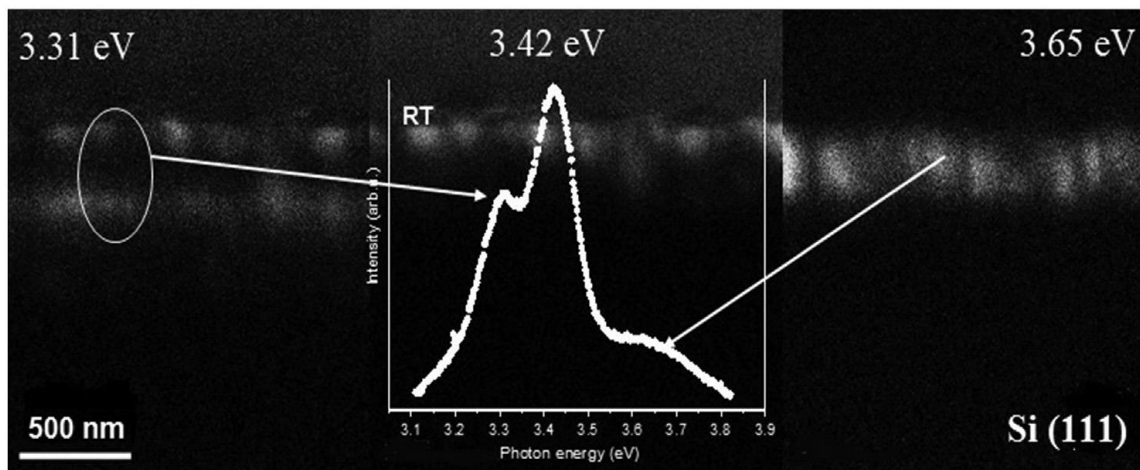


Fig. 10. Cross-sectional CL images for the 10-period MQW structure measured at RT [H8]

Having mastered the growth process of nanocolumns with single and multiple quantum wells on Si, we can study the shifting of the QWs caused by the quantum-confined Stark effect since, as it was mentioned before, the quantum structure grows in polar  $c$  direction.

### **Optical properties of ZnO/ZnMgO nanocolumns and planar structures and quantum wells located inside them, grown on $r$ -plane semi-polar sapphire substrates**

Intending to study the QCSE, I started with manufacturing the structures grown in non-polar  $a$  direction, to be taken as reference structures. As mentioned above, the non-polar structures can only be grown on  $r$ -plane semi-polar sapphire. The structure I created consisted of 5 ZnO quantum wells (1.5 nm - 3.483 eV, 2.5 nm - 3.449 eV, 3 nm - 3.426 eV, 4 nm- 3.416 eV and 6 nm - 3.360 eV) with ZnMgO barrier of 15 nm. The emission from these QWs is shown in Fig 11a. The position of PL peaks originating from the QWs can serve as a reference for QCSE studies, since there is no internal electric field present here. The spectrum also shows a clear emission from ZnMgO barrier (3.75 eV) and two phonon replicas (1LO, 2LO) [H5].

The structure of the samples is examined by the cross-sectional transmission electron microscopy (TEM). As it can be seen in Fig. 11b, the wells and the barrier layers can be clearly identified. The nominal thickness estimated based on laser reflectivity during growth

agree well with the values calculated from TEM image. The TEM image reveals uniformity across the entire structure.

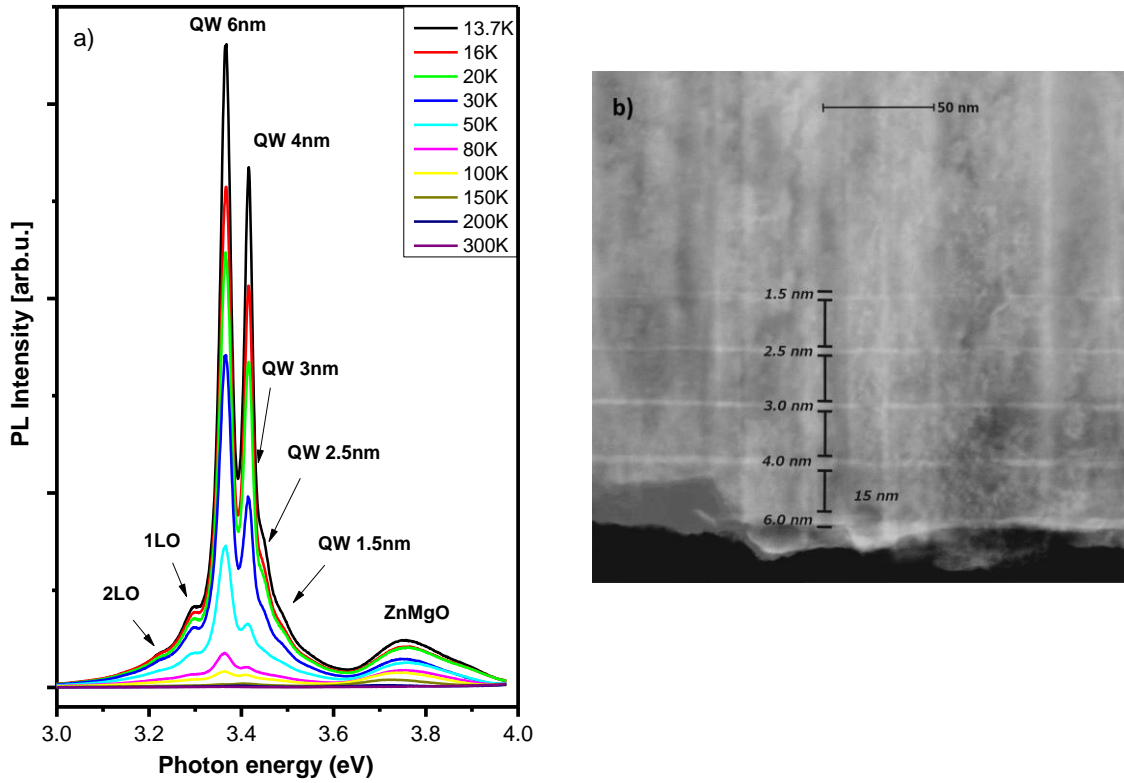


Fig.11. a) PL spectrum of a multi-well system of various widths b) TEM image of the cross-section of the structure grown on the *r*-plane  $\text{Al}_2\text{O}_3$  [H8]

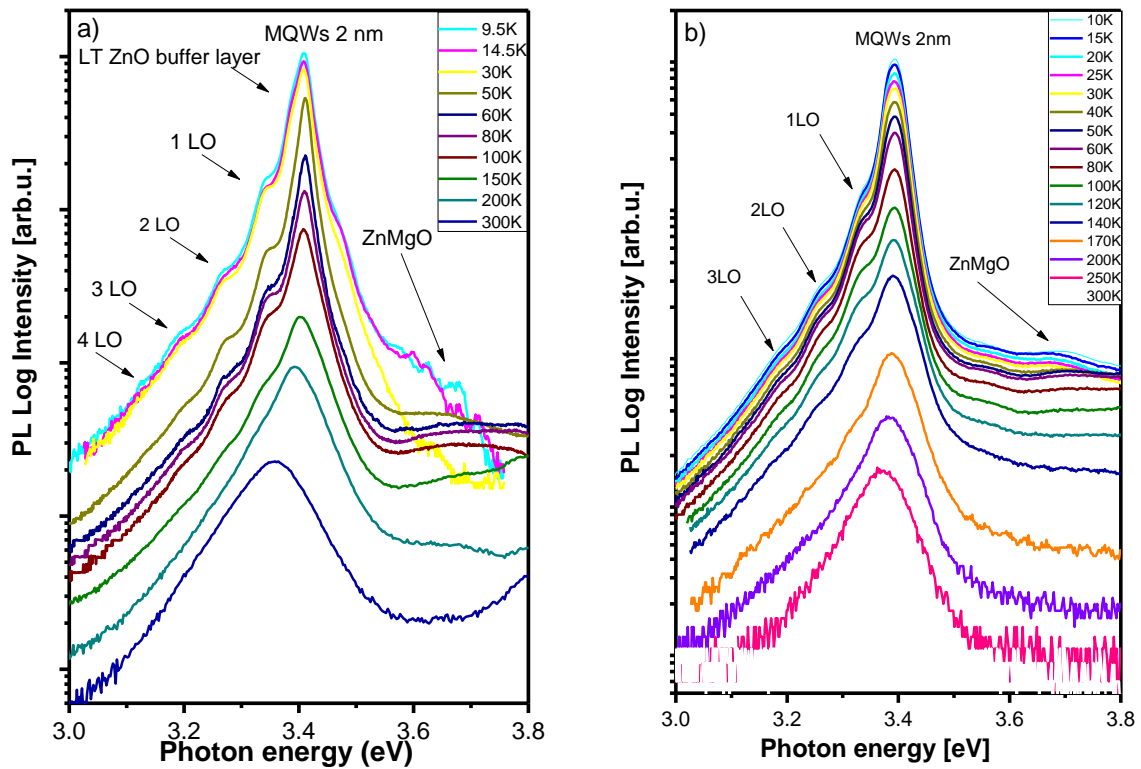


Fig. 12 Temperature dependence of MQWs grown on the *r*-plane  $\text{Al}_2\text{O}_3$  a) planar structure with a buffer layer b) nanocolumns without a buffer layer

The next step is examination of quantum wells located in planar structure and in nanocolumns. The fabricated ZnO/ZnMgO MQWs consist of 10 pairs of ZnO quantum wells (2 nm width) separated by 3 nm ZnMgO barrier, and such structures were created for both planar structure (see Fig. 1b) and nanocolumns (see Fig. 1a).

In Fig. 12a the PL spectra of a ZnO/ZnMgO structure grown on a ZnO buffer layer measured within a temperature range of 10– 300 K are shown. A sharp dominant peak, located at 3.406 eV, comes from the multiple QW structure particularly from recombination of excitons bound (BE) to neutral donors ( $D^0X$ ). We also observed a very weak peak at 3.383 eV, superimposed on the intense emission of MQWs. It is a near the band- edge (NBE) emission from the ZnO buffer. Emissions at 3.336 eV, 3.266 eV, 3.196 eV and 3.126 eV are also observed. These lines are interpreted, respectively, as originating from 1 LO, 2 LO, 3 LO and 4 LO phonon replica of the MQWs. The full width at half maximum (FWHM) value of the MQWs is ~39 meV at 7 K. In the higher energy part of the spectra a broad and faint peak with the maximum at about 3.650 eV, is recorded which is emission of the ZnMgO barrier. This emission of shifts to longer wavelength with increasing temperature, which is correlated with the band gap shrinkage. The PL intensity decreased very fast with increasing temperature, so since  $T=50K$  the spectra were measured with lower spectral resolution which influenced remarkably the shape of the PL spectra of ZnMgO. The PL from the ZnO buffer cannot be noticed above 50K, whereas the emission from the MQWs decays much slower and survives up to room temperature.

The temperature dependent PL spectra in range of 4.2 to 300 K are depicted in Fig. 12b. The spectrum measured at lowest temperature contains a sharp, dominant peak, located at 3.392 eV. It corresponds to recombination of excitons in the superlattice. The FWHM value of the MQWs at 10 K is ~40 meV. One can also find three weak peaks on the low energy tail of the main transition. The energy distance between them is 70 meV, so these can obviously be attributed to the first-, second- and third-order longitudinal optical (1LO, 2 LO and 3 LO) phonon replicas of the NBE emission from the superlattice. At the high energy part of the spectra a very weak peak at the maximum at about 3.700 eV is observed which we assign to the emission of ZnMgO barrier. The shift about 14 meV between the position of MQWs in the planar layer and nanocolumns is probably associated with a different content of Mg in the ZnMgO barrier layer. The energy position of excitonic transition in the 2 nm MQWs is lower than in case of quantum wells separated by thick barrier, here the barrier thickness is only 3 nm. The work of Zippel *et al.* [29] predicts that for this width of the barrier there exists the high probability of penetration of exciton wave functions to the barrier layers and interacting with the neighboring QW excitonic wave functions. In the case of MQWs it leads to lowering of the energy levels in the QW. The transition energy of the excitons localized in 2 nm thick QWs is much higher than in the case described above.

### **Optical properties of ZnO/ZnMgO nanocolumns and planar structures and quantum wells located inside them, grown on *c*-plane polar sapphire substrates**

Fig 13a presents an exemplary TEM image showing two ZnO quantum wells (1.5 and 4 nm width) separated by 15 nm ZnMgO barrier, in a single nanowire grown on *c*-plane sapphire substrate. Fig 13b we can see the PL spectrum of the structure described above. A strong emission from 2 ZnO/ZnMgO QWs (1.5 nm – 3.415 eV and 4 nm – 3.378 eV) is visible. There is also a clear luminescence from the ZnMgO barrier at 3.75 eV, what indicates the Mg content at about 20%, and four phonon replicas [H5]. Thus, we can observe the emission from

quantum wells located in a single nanowire. XRD measurements confirm that the ZnMgO structure grows in polar  $c$  direction.

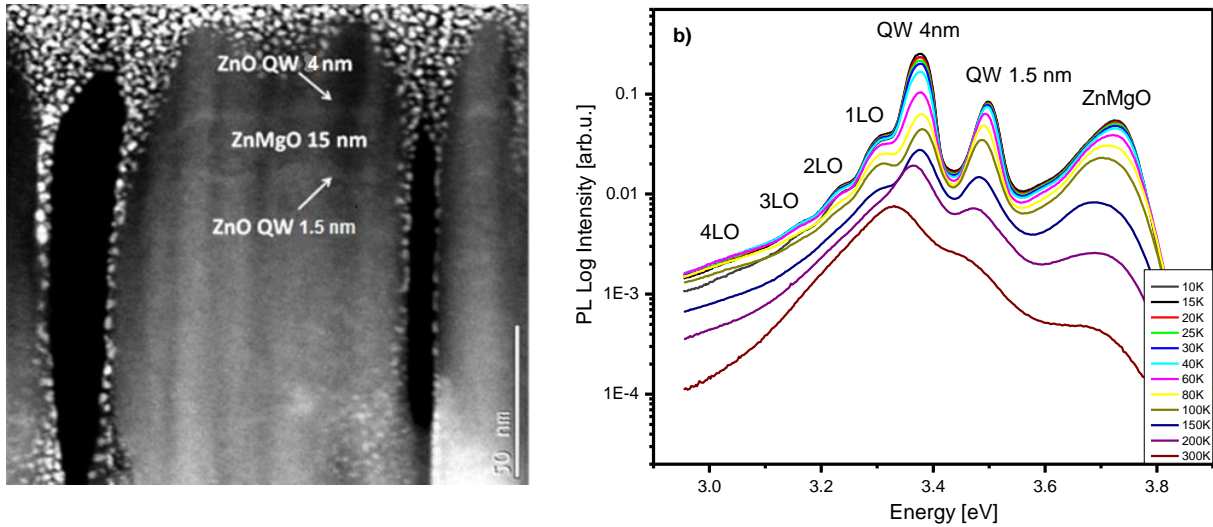


Fig 13. ZnO / ZnMgO quantum wells in ZnMgO nanocolumns a) image from TEM microscope b) PL spectrum measured at various temperatures [H5]

### Observation of quantum-confined Stark effect

During the growth process on polar  $c$ -plane substrate, we expect the shifting of luminescence spectra towards shorter wavelengths, due to the presence of strong internal electric fields. PL measurements of ZnO/ZnMgO quantum wells on sapphire substrates confirmed the occurrence of this effect [H5].

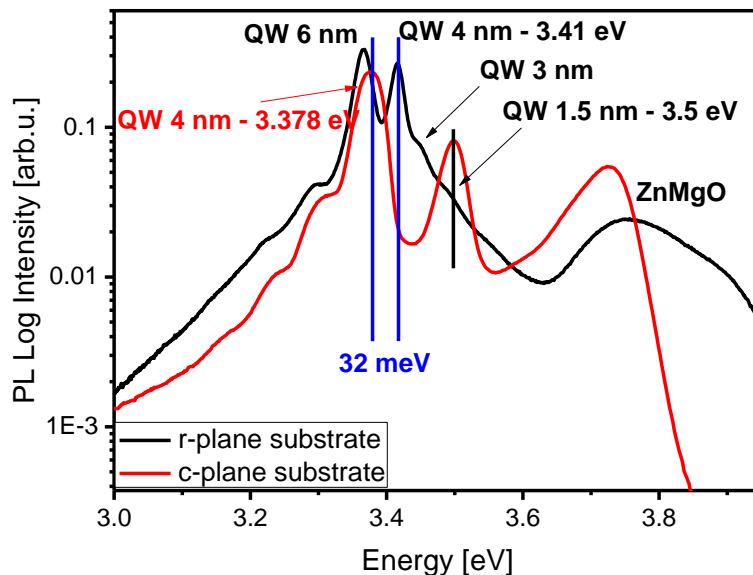


Fig. 14. Comparison of PL spectra of ZnO/ZnMgO quantum wells grown on different substrates [H5]

In Figure 14 we present the comparison of the PL spectra of ZnO/ZnMgO quantum structures grown on semi-polar substrate  $r$ -plane orientation (black curve) to the polar  $c$ - plane substrate (red curve). On the semi-polar substrate, the planar, non-polar,  $a$  oriented structure is obtained with the embedded quantum-wells of 1.5, 3, 4, 6 nm widths, while on the semi-polar substrate

the nanocolumns in the  $c$ - direction are grown. In these nanocolumns, two quantum wells were localized, of widths 1.5 and 4 nm. We compare the polar  $c$  structure with non-polar  $a$  structure. For the 1.5 nm quantum well no shift is observed, because the QW width is smaller than  $2 \cdot a_B$ . For a 4 nm QW, the spectrum is shifted 32 meV towards lower energies, due to the QCSE. The comparison of the luminescence spectra of ZnO/ZnMgO structures grown on the semipolar substrate with  $r$  orientation and on a polar  $c$ -oriented substrate is done. It is probably the first experiment comparing the QCSE for structures of different polarities ( $a$  and  $c$ ), grown on  $\text{Al}_2\text{O}_3$  substrates of different crystallographic orientations ( $r$  and  $c$ ) [H5].

### Study of the coupling of two asymmetric quantum wells

During my research, I studied the coupling between two asymmetric double quantum wells in internal electric field. If the distance between the QWs is small enough and the wavefunctions of trapped charges overlap, the tunnelling may occur. A system of coupled quantum wells may consist of two identical or two different (asymmetric) QWs. The coupling results in tunneling of excitons, or electrons and holes, to the wide well (it is an energetically favorable process), but on the other hand, the coupling causes a dramatic decrease of luminescence intensity, making it a very negative effect on luminescence efficiency. With the increase of barrier width, the tunnelling of the electrons is limited.

To study the coupling of asymmetric double ZnO/ZnMgO quantum wells, a commercial  $m$ -ZnO crystalline substrate was used. With this particular substrate, ideally lattice-matched, it was possible to fabricate planar structure of excellent quality and without any internal electric field.

Pairs of ZnO QWs 2 and 5 nm wide have been grown on ZnMgO buffer/barrier layers with Mg concentrations over 20%. The QWs are separated with 7 nm or 20 nm ZnMgO barriers. Temperature dependent photoluminescence and low temperature cross-sectional cathodoluminescence allowed to identify the origin of the observed spectral lines. Well resolved and narrow luminescence lines due to localized and free excitons are observed, confirming excellent quality of the structures. The PL measurements allowed to determine the binding energies of excitons in quantum wells which are  $\sim 55$  meV in 5 nm well and  $\sim 100$  meV in 2 nm well. The results of optical studies suggest that at the barrier width of 7 nm coupling between the wells enhances excitonic emission in 5 nm well via tunneling of charge carriers from 2 nm to 5 nm QW. No trace of inter-well coupling in a structure with a 20 nm thick barrier is observed.

One can therefore conclude that 7 nm is a maximum width for ZnMgO barrier separating ZnO QWs, for which the coupling was observed. the detailed description can be found in [H9].

[H2] presents a catalyst-free growth of ZnMgO nanocolumns in high temperature, with double asymmetric ZnO quantum wells (3 i 6 nm) separated by ZnMgO barriers of different widths (3 nm and 100 nm) deposited on Si (111). It was demonstrated that the 3 nm barrier ensures the coupling of QWs.

Two types of the Stark effect are possible in quasi-two-dimensional structures. The electric field may be applied parallel to or perpendicular to the growth axis. If the electric field is applied along the direction of growth, electrons and holes will be drawn into different quantum wells due to their opposite charges, and form spatially indirect excitons (IX). IX is a bound electron-hole pair separated by a thin barrier. IX in coupled quantum wells creates a unique system for the development of novel optoelectronic devices.

The close proximity of QWs allows the carriers to interact and form a bound state. The energy levels, binding energy and Bohr radius of IX can be calculated by different methods [30,31]. The spatial separation between the electron and hole layers allows one to control the overlap

of electron and hole WF and engineer structures with long IX lifetimes [32]. The binding energy of IXs is smaller than that of excitons in bulk ZnO, however it is large enough to make the IXs stable at room temperature [33].

To observe and investigate IX, double asymmetric ZnO/ZnMgO/ZnO quantum wells were grown on *a*-Al<sub>2</sub>O<sub>3</sub> substrates[H10]. Since, as mentioned above, on these substrates the layer grows in the polar *c* direction, an internal electric field is present.

We have studied structures consisting of QWs of different widths: (3 and 5 nm) separated by a 12 nm ZnMgO barrier (structure # 1), a 2.5 nm barrier (structure # 2) and a structure with 2 and 4 nm wells with a 2.5 nm ZnMgO barrier (structure # 3). The QWs were wide enough for the Stark effect to be observed. The internal electric field in these structures is directed in the *c* direction (direction of growth), and as a result the quantum wells are tilted.

All the calculations presented here were made by Dr Janusz Andrzejewski from the Wroclaw University of Technology. For single-particle transitions – electrons and holes – the 8 *k*-*p* model for structure of wurtzite is used, with accounts not only for the potential resulting from discontinuities in the conductivity and valence bands caused by the different layers of the material, but also for strain effects and spontaneous polarization. The variational approach was used to describe the excitons, where the so-called one-parameter 2D-dimensional hydrogen-like wave function was used to describe the relative movement electron and hole, and the one-particle wave functions from the 8 *k*-*p* model were used to describe the electron and hole behavior.

Integrating the excitonic Hamiltonian using the wave function constructed in this way, with the exception of one variable describing the motion of either an electron or a hole, we obtain equations that differ from single-particle equations – there is an additional Coulomb potential resulting from the transverse mutual movement of the electron and the hole.

To solve the set of equations complicated as this, we use the self-consistent field method – as a result, we obtain equivalents of single-particle wave functions for electrons and holes, as well as the effective potential that includes the aforementioned Coulomb potential. Structure #1 was taken as a reference structure. In this asymmetric system, the energies of the direct excitons of the QWs are well separated, which considerably facilitates the interpretation of the optical spectra. The calculated electric fields have values 0.0068 MV/cm and 0.25 MV/cm in the barrier and in both QWs, respectively.

The structure #2 that will be studied is formed by two ZnO quantum wells with the same widths (4 and 5 nm) as in the previous structure, the ZnMgO barrier between the QWs is thinner and equal to 2.5 nm. The barrier layer is sufficiently thin to allow charges to the tunnel between the QW layers. Incidentally, the electrons initially created in one of the wells can tunnel to the second well and form a two-dimensional gas of spatially IX. In structure #2, due to a lower concentration of Mg (9%) in QWs than the previous structure #1 (Mg = 10%), the electric field in QWs has slightly lower value 0.23 MV/cm with the 0.0062 MV/cm strength in the barrier.

Structure #3 consists of double quantum wells (4 nm and 2 nm) and a ZnMgO barrier with thickness of 2.5 nm. In this structure, the electric fields in QWs are very similar to structure #2, but with a lower value of 0.0042 MV/cm in the barrier.

The geometry of structures #1 and #2 is very similar – they differ only in the width of the barrier. So we see the similarity of the PL spectra of both these structures, which is confirmed by calculations. We observed the same single particle transitions in both asymmetric quantum wells (3.358 - 5 nm and 3.383 - 4 nm) and the same exciton energy FX (3.4 eV).

In structure #2, an additional transition is observed, denoted A, and it is the direct exciton EL2 in the QW 4nm region, denoted by Direct EL2 in Table 1 (Fig. 15). Due to the interaction of

the electric field and the barrier width, this type of exciton could not be observed in structure #1.

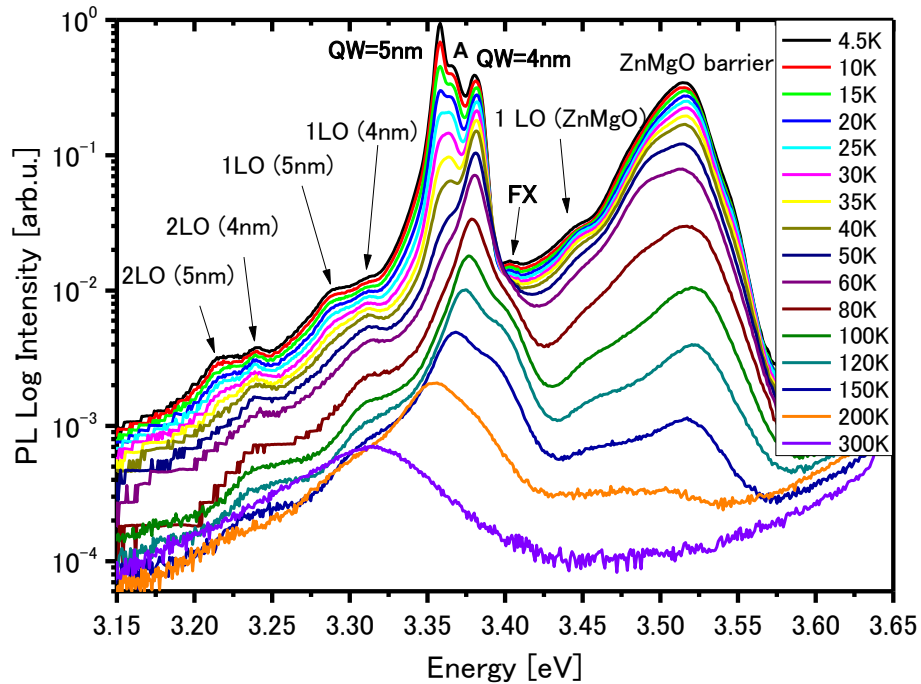


Fig. 15. The PL spectrum measured at different temperatures for a structure with two asymmetric quantum wells (4 nm and 5 nm) and a ZnMgO barrier with a thickness of 2.5 nm [H10].

Structure #3 is quite similar to structure # 2 - it has the same ZnMgO barrier width (2.5 nm) and has one quantum well (4 nm) of the same width as the previous structure. The difference between these structures is due to the difference in the width of the second quantum well (2 nm).

The emission at 3.382 eV, as in all previous cases, is attributed again to ground-state transitions in QW 4nm. The peak at 3.405 eV can be interpreted as transitions between the energy levels of the first electron and the second hole in QW 2nm. The peak energy of 3.431 eV (denoted by FX), which, similarly to structures # 1 and # 2, we attribute to the extended exciton EL1 - the exciton in which the wave function is very weakly bound in the well (Table 1). In structure #3, the wider QW is 4 nm wide, while in structures # 1 and # 2 it is 5 nm wide, so the FX peak is shifted towards higher energies (Fig. 16).

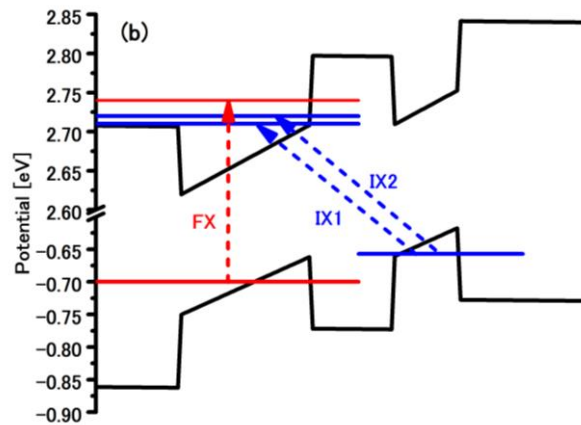
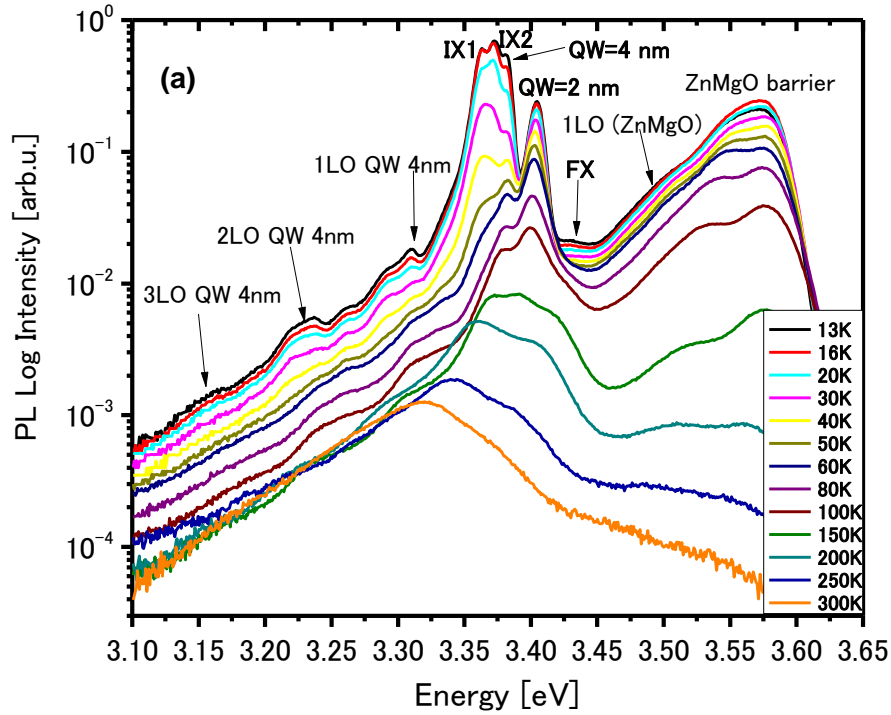


Fig. 16. a) PL spectrum measured at different temperatures for a structure with two asymmetric quantum wells (2 nm and 4 nm) and a 2.5 nm ZnMgO barrier b) schematic diagram of indirect excitons (IX1 and IX2 - blue dashed line) and FX (red dashed line) [H10].

On the lower energy side of the ground state transitions in QW 4nm we observed two additional peaks at 3.364 eV (marked by IX1) and 3.372 eV (marked by IX2) (Fig.16a). These two peaks could be attributed to indirect exciton—Table 1. Energies of all these three excitons are presented by schematic diagram on the second panel in Figure 16b.

Exciton energy [eV]	Binding energy [meV]	Oscillator strength	Description
3.324	13.45	0.00	Indirect EL1@QW4nm-HH1@QW2nm
3.347	33.10	0.488	Direct EL1@QW4nm-HH1@QW4nm
3.361	6.856	0.001	Indirect EL2@QW4nm-HH1@QW2nm
3.372	6.796	0.001	Indirect EL3@QW4nm-HH1@QW2nm
3.399	15.34	0.397	Direct EL1@QW2nm-HH1@QW2nm
3.413	19.36	0.260	Direct EL2@QW2nm-HH1@QW2nm
3.427	11.18	0.160	Extended EL1 above QW4nm-HH1@QW4nm
3.443	14.10	0.111	Extended EL2 above QW4nm-HH1@QW4nm
3.474	14.88	0.081	Indirect EL1@QW2nm-HH1@QW4nm

Table 1. Calculated exciton energy, binding energy and oscillator strength in the 8  $k_p$  model for different types of excitons observed in structure #3 [H10].

The electron and hole multipliers for the indirect EL2 exciton are presented in Figure 17 (for indirect EL3 exciton, the electron (a) and hole (b) multipliers are very similar). The electron multiplier for indirect EL2 exciton (Fig. 17a) in structure #3, and for extended EL1 exciton in structure #1, are both expanded into the barrier/cap layer, but the former electron multiplier has only two nodes whereas the latter has many more nodes. This indicates that the electron factor of the exciton WF is more confined for the indirect than for the direct exciton, so despite the very weak oscillator strength, the transition for the indirect exciton in this structure #3 could be seen.

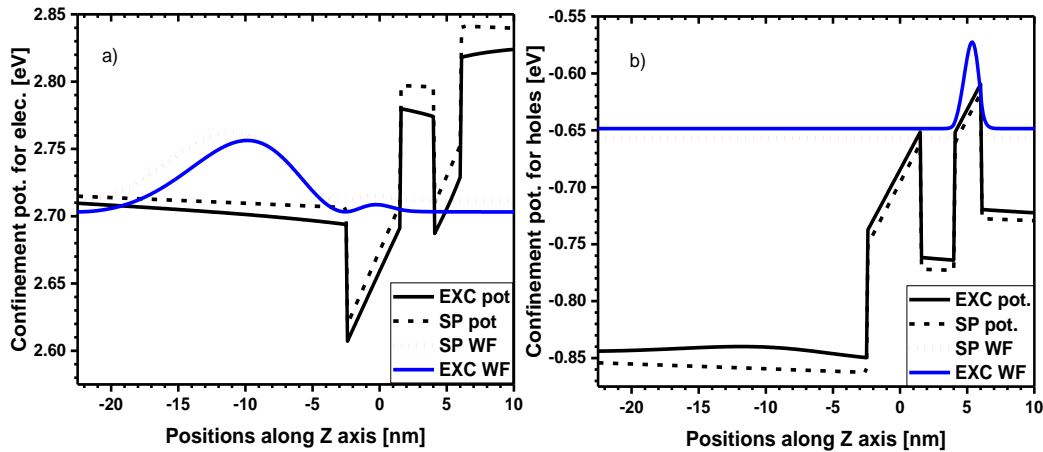


Fig. 17. Potentials of the conductivity band (Fig. 17a) and the valence band (Fig. 17b) for the exciton, including the additional Coulomb term (black solid line) and single-particle potentials (black dotted line). The continuous blue line marks the electron (Fig. 17a) and the hole (Fig. 17b) part of the wave function for the EL2-type indirect exciton. The red dashed line shows the corresponding one-particle wave functions for the electron and the hole [H10].

### Optical properties of ZnO/ZnCdO multiple quantum wells in ZnO nanowires, grown on Si(111)

The structure described in [H7] consists of 30 periodic ZnCdO/ZnO MQWs. The width of both QWs and barriers was 2 nm.

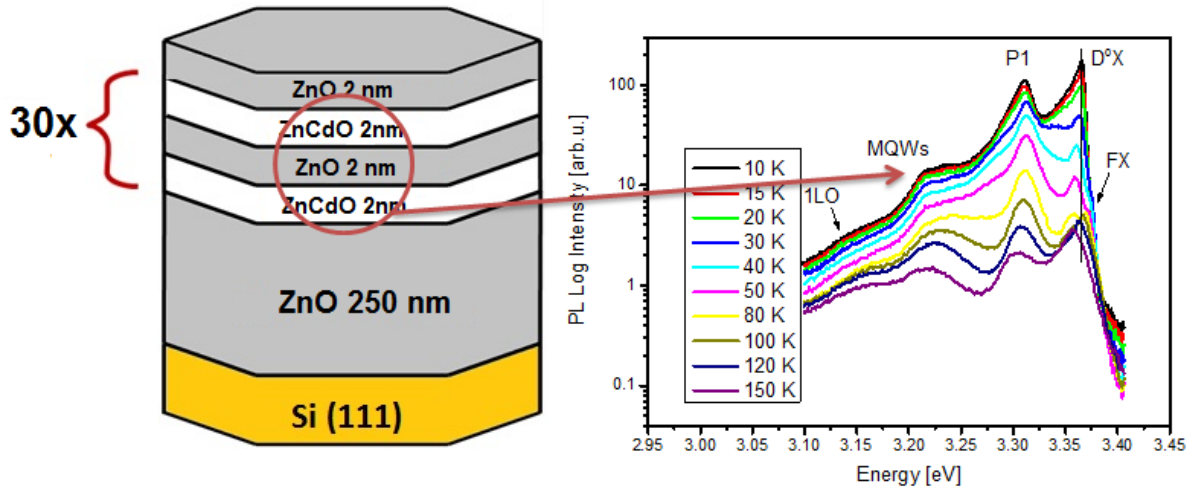


Fig. 18. Diagram of the sample and the temperature dependence of PL for the ZnO/ZnCdO structure [H7]

At low temperatures, near band edge luminescence as well as blue emission dominates. A peak centered at 3.365 eV at 10 K can be attributed to the emission of excitons bound to neutral donors  $D^0X$  (Fig.18). With increasing temperature, the  $D^0X$  peak gradually shifts towards lower energies, from 3.365 eV at 10 K to about 3.356 eV at 100 K, then disappears and becomes undetectable at temperatures above 120 K. Free exciton emission (FX) at 3.375 eV at 10 K is also observed. The FX band appears as a shoulder at the higher energy side of the  $D^0X$  peak. The FX emission becomes dominant with a further temperature increase (at temperatures higher than 100 K) and gradually shifts to lower energies. The effect of emission switching from  $D^0X$  to FX is typical for oxide structures, as I have mentioned before. The band at 3.31 eV (P1) is commonly observed in the emission spectra of various ZnO samples. Tainoff *et al.* [34] suggested that the 3.31 eV emission results from a defect-related transition and its appearance was ascribed to a free-to-bound (FB) transition [34]. The activation energy of the aforementioned PL band was found to be equal to  $122 \pm 5$  meV. The authors of that paper claim that the corresponding defect might be of crystalline origin since its presence has been observed in various kinds of ZnO samples, structured at different scales: a single crystal (macroscale), a microcrystalline powder (mesoscale), and an assembly of ZnO nanoparticles (nanoscale) [34]. Emission at 3.21 eV can be attributed to the exciton confined in ZnCdO/ZnO wells. As the temperature increases from 10 to 50 K, we observe the blue shift of the peak position and from 80 to 150 K the peak position's red shift. It is probably an effect of slightly disordering between the ZnCdO well and ZnO barriers.

## Conclusions and summary

Main goals and achievements:

1. Fabrication of high quality ZnMgO nanocolumns with MBE technique on Si(111) and sapphire substrates, with various orientations and polarities ( $c$ ,  $r$ ), directly on a clean surface, with and without application of the buffer layer [H1, H2, H4, H5]
2. Fabrication of quantum wells, multiple QWs and ZnMgO/ZnO/ZnMgO super-lattices in a single ZnMgO nanocolumn [H2, H3, H4, H5, H8].
3. Estimation of the liminal width of the ZnMgO barrier, for which we can observe the overlapping of QW wave functions, and the tunnelling of charge carriers [H2, H9].
4. Study of the quantum-confined Stark effect for QWs fabricated on substrates with structures grown in polar direction [H5].

5. Study of the indirect exciton (IX) in planar structures grown on  $\alpha$ -Al<sub>2</sub>O<sub>3</sub> substrate [H10].
6. Description of growth process of nanostructures (nanowalls) directly on clean (without a catalyst) commercially available 4H-SiC substrates [H6].
7. Study of ZnO/ZnCdO nanostructures grown with MBE technique on silicon surfaces, without a catalyst, in very low temperature of deposition [H7]

The results presented in the compilation of works constituting the basis for the habilitation thesis pertain to the optimization of MBE growth of ZnO-based quantum structures, and investigation of optical and structural properties of quantum wells located in these nanostructures.

The vast majority of structures were grown on silicon. Silicon, while easily available and cheap, has also a number of drawbacks, like fast oxidation of the surface, and large lattice mismatch compared to ZnO. These problems have been successfully solved, and thus (properly tuning the growth conditions, temperature and thickness of the buffer layer) we can obtain monolythic layers of any thickness and nanocolumns with diameter about 30-50 nm. It was demonstrated that the temperature of the buffer layer affects the diameter of the nanocolumns. MBE growth procedures for Zn(Mg,Cd)O on silicon are particularly important, since very few scientific groups have dealt with this problem so far. Sallet *et al.* [11] mentions substantial difficulties of catalyst-free growth, emphasizing that [H1] is the only work where the ZnMgO nanocolumnar structures, grown by MBE without any catalyst, were presented. Similar effects can also be achieved on 4H-SiC and sapphire substrates with various orientations and polarities, where a number of nanostructures can be fabricated by selecting a right set of growth conditions. It is clearly apparent, that nanocolumnar growth occurs in nonstoichiometric conditions.

The results of the studies of ZnO/ZnMgO quantum structures demonstrate that the MBE technique of obtaining of these structures was indeed fully mastered. A careful control of widths of barriers between quantum wells in double and multiple QW systems allowed to observe the effect of narrow QW luminescence damping induced by a neighboring wide quantum well. This effect is reflected in decrease of the exciton lifetime in narrow quantum well.

The ZnO/ZnMg(Cd)O quantum wells (single, double and multiple) of different sizes and different widths of ZnMgO barrier were localized in the nanostructures. Their interactions were studied according to the barrier width, and thus a critical thickness of the barrier was established, for which the interaction still exists. In these experiments, a commercial m-ZnO crystal substrate was used to avoid any internal electric fields, and to obtain a structure with high crystalline quality. It appears that 7 nm is the maximum ZnMgO barrier width for double asymmetric ZnO/ZnMgO quantum wells located in planar structure.

The effect of the QWs interaction on luminescence spectrum was also described. It is a rather important issue, since it may be used e.g. for ZnO/ZnMgO-based lasers design.

Comparative studies of asymmetric quantum double wells of different widths and with different ZnMgO barriers, grown on Al<sub>2</sub>O<sub>3</sub> substrates using PL, were also carried out. The PL analysis was supported by the theory where an 8-band  $k\cdot p$  model of the wurtzite structure for single particle states was used. By partial integration of the exciton wave function, additional potentials appear and using the so-called self-consistent field theory, this potential was calculated.

In the structure with two ZnO quantum wells (of widths 2 nm and 4 nm) with a 2.5 nm ZnMgO barrier, indirect excitons IX1 and IX2 were observed.

Moreover, the electric experiments performed on samples I fabricated, contributed to some parts of a PhD thesis, three Master's dissertations and one engineer dissertation still in progress. All these works were realized in Wrocław University of Science and Technology.

#### 4.4 Bibliography

- [1] Ü. Özgür, Y.I. Alivov, C. Liu, M.A. Reshchikov, S. Dogan, V. Avrutin, S.J. Cho, H. Morkoc, *J. Appl. Phys.* 98 (2005) 041301
- [2] X. Yu, T. J. Marks, A. Facchetti, *Nat. Mater.* 15 (2016) 383–396.
- [3] Y. Qin, X. Wang, L.Z. Wang, *Nature* 451 (2008) 809–813.
- [4] H. Morkoç, Ü. Özgür, *Zinc Oxide: Fundamentals, Materials and Device Technology*, 1st ed.; WILEY-VCH Verlag GmbH & Co. KGaA:Weinheim, Germany, 2009.
- [5] M. Borysiewicz, *Crystals* 9 (2019) 505
- [6] A. Singh, D. Kumar, P.K. Khanna, M. Kumar, B. Prasad, *ECS J. Solid State Sci. Technol.* 2 (2013) Q136–Q141,
- [7] W.I. Park, G.-C. Yi, H. Jang, *Appl. Phys. Lett.* 79 (2001) 2022
- [8] J.M. All Abbas, P. Narin, E. Kutlu, S.B. Lisesivdin, E. Ozbay, *Phys. B Condens. Matter* 556 (2019) 12–16,
- [9] J. Agrawal, T. Dixit, I.A. Palani, M.S.R. Rao, V. Singh, *J. Phys. D Appl. Phys.* 51 (2018) 185106.
- [10] S. Riyopoulos, *Nanoscale Res. Lett.* 4 (2009) 993-1003
- [11] T. Takeuchi, C. Wetzel, S. Yamaguchi, H. Sakai, H. Amano, I. Akasaki, Y. Kaneko, S. Nakagawa, Y. Yamaoka, N. Yamada, *Appl. Phys. Lett.* 73 (1998) 1691
- [12] P. Perlin, C. Kisikowski, V. Iota, B.A. Weinstein, L. Mattos, N.A. Shapiro, J. Kruger, E. R. Weber, J. Yang, *Appl. Phys. Lett.* 73 (1998) 2778
- [13] P. Hille, J. Mussener, P. Becker, M. de la Mata, N. Rosemann, C. Magen, J. Arbiol, J. Teubert, S. Chatterjee, J. Schormann, M. Eickhoff, *Appl. Phys. Lett.* 104 (2014) 102104.
- [14] N. A. Shapiro, P. Perlin, C. Kisielowski, L.S. Mattos, J. W. Yang, E. R. Weber, *MRS Internet J. Nitride Semicond. Res.* 5 (2000) 1
- [15] V. Sallet, C. Deparis, G. Patriarce, C. Sartel, G. Amiri, J-M. Chauveau, C. Morhain, J. Z. Perez *Nanotechnology* 31 (2020) 385601
- [16] A. Wierzbicka, Z.R. Zytewicz, S. Kret, J. Borysiuk, P. Dluzewski, M. Sobanska, K. Klosek, A. Reszka, G. Tchutchulashvili, A. Cabaj, E. Lusakowska, *Nanotechnology* 24 (2013) 035703
- [17] T. Aschenbrenner, C. Kruse, G. Kunert, S. Figge, K. Sebald, J. Kalden, T. Voss, J. Gutowski, D. Hommel, *Nanotechnology* 20 (2009) 075604
- [18] Y. Chen, H.-J. Ko, S.-K. Hong, T. Yao, *Appl. Phys. Lett.* 76 (2000) 559-561.
- [19] M.W. Cho, A. Setiawan, H.J. Ko, S.K. Hong, T. Yao, *Semicond. Sci. Technol.* 20 (2005) S13
- [20] D. Look, *Mater. Sci. Eng. B* 80 (2001) 383
- [21] S. Yoshida, Band structure of SiC: overview *Properties of Silicon Carbide* ed Z C Feng and J H Zhao (London: INSPEC, the Institution of Electrical Engineers) (1995) 74–80
- [22] Z.C. Feng, J.H. Zhao, *Silicon Carbide: Materials, Processing, and Devices* 20 (2004) 2–34
- [23] M. Gammon, A. Perez-Tomas, M.R. Jennings, G.J. Roberts, M.C. Davis, V.A. Shah, S.E. Burrows, N.R. Wilson, J.A. Covington, P.A. Mawby, *Appl. Phys. Lett.* 93 (2008) 112104
- [24] H.P. He, Y.Z. Zhang, Z.Z. Ye, H.H. Huang, X.Q. Gu, L.P. Zhu, B.H. Zhao, *J. Phys. D: Appl. Phys.* 40 (2007) 5039.
- [25] <http://www.epitaxyproject.com/>

- [26] K.J. Button, D.R. Cohn, M. von Ortenbert, B. Lax, E. Mollwo, R. Helbig, *Phys. Rev. Lett.* 28 (1972) 1637-1639.
- [27] K. Hummer K, *Phys. Status Solidi B* 56 (1973) 249-260
- [28] K. Wu, H. He, Y. Lu, J. Huang, Z. Ye, *Nanoscale* 4 (2012) 1701-1706.
- [29] J. Zippel, M. Stölzel, A. Müller, G. Benndorf, M. Lorenz, H. Hochmuth, M. Grundmann, *Phys. Status Solidi B* 247 (2010) 398-404.
- [30] M.H. Szymanska, P.B. Littlewood, *Phys. Rev. B* 67 (2003) 193305
- [31] S. de-Leon, B. Laikhtman, *Phys. Rev. B* 61 (2000) 2874
- [32] L.V. Butov, *Superlattices Microst.* 108 (2017) 2-26
- [33] Y.Y. Kuznetsova, F. Fedichkin, P. Andreakou, E.V. Calman, L.V. Butov, P. Lefebvre, T. Bretagnon, T. Guillet, M. Vladimirova, C. Morhain, J.-M. Chauveau, *Opt. Lett.* 40 (2015) 3667
- [34] D. Tainoff, B. Masenelli, P. Mélinon, A. Belsky, G. Ledoux, D. Amans, C. Dujardin, N. Fedorov, P. Martin, *Phys. Rev. B* 81 (2010) 115304-8.

## 5. Information on scientific activity

### 5.1 Description of scientific output not related to the habilitation thesis before obtaining a Ph. D. degree in physics

As part of my Master degree work, completed in Silesian University of Technology in Gliwice (Faculty of Mathematics and Physics) under supervision of Professor Marian Urbańczyk, I performed the measurements of sensor properties using the surface acoustic waves. The results of this studies were in part published in [N1], presenting the measurements of changes of the resistance of the phthalocyanine and palladium bilayer sensor structure induced by medium hydrogen concentrations (0.5–4%) in nitrogen and air. The title of my Master’s dissertation was: Elektryczne i akustyczne badanie dwuwarstwowych struktur sensorowych („Electrical and acoustic study of two-layer sensor structures”).

After completing my Master’s degree, I studied for my PhD in PAN Institute of Physics. My PhD thesis was dedicated to investigating the electronic structure of GeTe and PbTe-based compounds with Mn and/or selected rare earth elements (Eu, Gd), using Resonant Photoemission Spectroscopy. Thus, I studied the crystals that after introduction of transition metals become (or, according to some theories, may become) semimagnetic or ferromagnetic semiconductors.

The information about the contribution of 3d and 4f states in valence band of these compounds was significant. The  $A^{IV}B^{VI}$  compounds I studied have an important practical application i.a. in infrared lasers used in fiber optics or as a thermoelectric materials. They are characterized by some unique properties, e. g. high dielectric constant. All the results included in PhD dissertation were measured in Hamburg (HASYLAB) and Lund (Max-Lab) synchrotrons. A detailed description can be found in the doctoral dissertation [N2] and in the works [N3-N21].

In cooperation with Laboratoire de Physique des Matériaux Electroniques in Namur, Belgium, studies on the interaction of Mn thin layers on GaN (000-1) surface were carried out using a scanning tunneling microscope and a secondary ion mass spectrometer with a time-of-flight analyzer. The cooperation resulted in work [N22].

[N1] W.P. Jakubik, M.W. Urbanczyk, J. Bodzenta, **M.A. Pietrzyk**, *Investigations on the resistance of metal-free phthalocyanine and palladium bilayer sensor structure influenced by hydrogen*, Sensor. Actuator. B-Chem, 105, 340-345 (2005)

[N2] **M. A. Pietrzyk**, *Wkład otwartych powłok 3d i 4f do struktury elektronowej wybranych półprzewodników IV-VI z Mn, Gd i Eu*. Praca doktorska, Warszawa 2010

[N3] B.A. Orlowski, B.J. Kowalski, P. Dziawa, **M. Pietrzyk**, S. Mickievicius, V. Osinniy, B. Taliashvili, I.A. Kowalik, T. Story, R.L. Johnson, *Fano resonance of Eu<sup>2+</sup> and Eu<sup>3+</sup> in (Eu,Gd)Te MBE layers*, Acta Phys. Pol. A 803, 108 (2005)

[N4] B.J. Kowalski, B.A. Orlowski, **M. Pietrzyk**, P. Kaczor, K. Kopalko, S. Mickievicius, R.L. Johnson, *Band Structure of Mn/ZnTe Studied by Angle-Resolved Photoelectron Spectroscopy* – Acta Phys. Pol. A 735, 108 (2005)

[N5] B.A. Orlowski, P. Dziawa, B. Kowalski, I. Kowalik, **M. Pietrzyk**, V. Osinniy, T. Story, S. Mickievicius, R. Johnson, *Resonant photoemission study of Eu<sub>1-x</sub>Gd<sub>x</sub>Te layers*, Appl. Surf. Sci, 252, 5379 (2006)

[N6] B. J. Kowalski, **M.A. Pietrzyk**, B.A. Orlowski, P. Dziawa, V. Osinniy, J. Pelka, W. Dobrowolski, V.E. Slynko, E.I. Slynko, R.L. Johnson, *Photoemission study Ge<sub>1-x-y</sub>Mn<sub>x</sub>Eu<sub>y</sub>Te at Mn 3p-3d and Eu 4d-4f resonances*, J. Electron. Spectrosc. Relat. Phenom, 156, 315 (2007)

[N7] P. Dziawa, B.A. Orlowski, V. Osinniy, **M. Pietrzyk**, B. Taliashvili, T. Story, R. L. Johnson, *Photoemission study of Eu<sup>2+</sup>/<sup>3+</sup> ions In ferromagnetic (Eu, Gd) Te semiconductor layers*, Material Science- Poland 25, 2 (2007)

[N8] B.A. Orlowski, B.J. Kowalski, **M. Pietrzyk**, S. Mickievicius, V. Osinniy, P. Dziawa, T. Story, W. Drube, R.L. Johnson, *Photoemission study of (PbEuGd)Te layers under Gd or Te atoms treatment*, J. Electron. Spectrosc. Relat. Phenom, 156, 315 (2007)

[N9] **M.A. Pietrzyk**, B.J. Kowalski, B.A. Orlowski, W. Knoff, V. Osinniy, I.A. Kowalik, T. Story, R.L. Johnson, *Photoemission study of Mn 3d electrons in the valence band of Mn/GeMnTe*, Acta Phys. Pol. A, 112, 275 (2007)

[N10] S. Mickevicius, V. Bonderka, S. Grebinskij, A.K. Oginskis, R. Butkute, H. Tvardauskas, B. Vengalis, B.A. Orlowski, V. Osinniy, **M.A. Pietrzyk**, W. Drube, *The metals valence states in La<sub>0.7</sub>Ce<sub>0.3</sub>MnO<sub>3</sub> thin films*, Acta Phys. Pol. A 113, 1071 (2008)

[N11] **M. A Pietrzyk**, B. A. Orlowski, B. J Kowalski, P. Dziawa, V. Osinniy, T. Story, B. Taliashvili, R. L. Johnson, *Resonant photoemission studies of Gd/PbGdTe*, J. Phys. Conf. Ser. 100, 072015 (2008)

[N12] B.A. Orlowski, V. Osinniy, P. Dziawa, **M. Pietrzyk**, B.J. Kowalski, B. Taliashvili, T. Story, R. L. Johnson, *Fano resonance investigation of PbTe layers containing Eu and Gd ion*, Acta Phys. Pol. 114, 351-6 (2008)

[N13] B.A. Orlowski, B.J. Kowalski, **M.A. Pietrzyk**, R. Buczko, *Resonant Photoemission Study of 4f Electrons on the Surface of Semiconductors*, Acta Phys. Pol. 114, S-103 (2008)

[N14] **M.A. Pietrzyk**, B.J. Kowalski, B.A. Orlowski, P. Dziawa, W. Knoff, V. Osinniy, I.A. Kowalik, W. Dobrowolski, V.E. Slynko, E.I. Slynko, R.L. Johnson, *Electronic structure of bulk ferromagnetic  $Ge_{0.86}Mn_{0.14}Te$* , Radiat. Phys. Chem. 78, S17-S21 (2009)

[N15] B.A. Orlowski, **M.A. Pietrzyk**, V. Osinniy, M. Szot, E. Lusakowska, K. Graszka R.L. Johnson, *Photoemission study of 6H-SiC (0001) surface with deposited Mn atoms*, Radiat. Phys. Chem. 78, S17-S21 (2009)

[N16] B.A. Orlowski, B.J. Kowalski, E. Guziewicz, E. Lusakowska, V. Osinniy, I.A. Kowalik, **M.A. Pietrzyk**, E. Nossarzewska-Orlowska, R.L. Johnson, *Microscopic (AFM) and resonant photoemission study of Gd/Si (111) interface*, Radiat. Phys. Chem, 78, S22-S24 (2009)

[N17] B.J. Kowalski, **M.A. Pietrzyk**, W. Knoff, A. Łusakowski, J. Sadowski, J. Adell, T. Story, *Angle-resolved photoemission study and pseudopotential calculations of GeTe and  $Ge_{1-x}Mn_xTe$  band structure*, Physcs. Proc. 3, 1357 (2010)

[N18] **M.A. Pietrzyk**, B.J. Kowalski, B.A. Orlowski, W. Knoff, T. Story, W. Dobrowolski, V.E. Slynko, E.I. Slynko, R.L. Johnson, *A comparison of the valence band structure of bulk and epitaxial GeTe-based diluted magnetic semiconductors*, Acta Phys. Pol. 117, 293 (2010)

[N19] B.A. Orlowski, A. Szczerbakow, B.J. Kowalski, **M.A. Pietrzyk**, K. Gas, M. Szot, W. Szuszkiewicz, V. Domukhovski, S. Mickevicius, R.L. Johnson, S. Thiess, W. Drube, *Photoemission spectra of frozen rock salt  $Pb_{1-x}Cd_xTe$  crystal*, J. Electron. Spectrosc. Relat. Phenom. 184,199 (2011)

[N20] **M.A. Pietrzyk**, B.A. Orlowski, B.J. Kowalski, P. Dziawa, V. Osinniy, B. Taliashvili, R.L. Johnson, *Fotoemisyjne badania gadolinu osadzonego na czystej powierzchni PbGdTe*, Biuletyn Polskiego Towarzystwa Promieniowania Synchrotronowego 5, 204 (2006)

[N21] V. Osinniy, B.A. Orlowski, P. Dziawa, B.J. Kowalski, **M.A. Pietrzyk**, B. Taliashvili, S. Mickevicius, T. Story, R.L. Johnson, *Badania fotoemisji rezonansowej warstw (Eu,Gd)Te/Te*, Biuletyn Polskiego Towarzystwa Promieniowania Synchrotronowego 5, 213 (2006)

[N22] J. Dumont, B.J. Kowalski, **M. Pietrzyk**, T. Seldrum, L. Moussiau, B. Douhard, I. Grzegory, S. Porowski, R. Sporken, *Atomically flat GaMnN by diffusion of Mn into GaN (0001)*, Superlattices Microst. 40, 607-611 (2006)

## **5.2 Description of scientific achievements not related to the topic of habilitation, after obtaining the PhD**

After completing my PhD, I was employed in PAS Institute of Physics, joining the group of MBE growth of oxide nanostructures. There, apart from the studies described in this dissertation, I participated in research on obtaining the p-type conduction in ZnO layer by group V element doping, and I also worked on application of ZnO-based junctions for selective detection of UV radiation [D1-D4]. I was also involved in studies of interdiffusion in single and multiple ZnO/ZnMg(Cd)O quantum wells [D5, D6].

Apart from the research described above, the structures I fabricated were also used for other purposes. Studies of strain relaxation depending on the Mg content were performed, for both

nanocolumns and planar ZnMgO structures grown on *a*-plane sapphire. The Mg content in the structures was studied using the RBS method, and the exact determination of the crystal lattice parameters was performed using the HR XRD technique. It is a non-destructive technique that gives the correct values of the strain distribution. We observe a gradual increase of stress with the increase in Mg content in the ZnMgO layers, in particular in the *c* direction. For high Mg content, high values of the tilt and twist angles were obtained. The epitaxial layer  $\text{Mg}_x\text{Zn}_{1-x}\text{O}$  containing 32.9% Mg has lower structural quality, which may result from worse incorporation of the impurity into the lattice. The obtained results show a non-linear relationship between the lattice parameters and the Mg content. Increasing the Mg content leads to a residual increase in the value of in-plane and out-of-plane strains. A detailed description and interpretation can be found in [D7].

Furthermore, as a collaboration with Wrocław University of Science and Technology, I participated in Raman spectroscopy measurements, evaluating the crystalline quality of the obtained structures and monitoring the strain in ZnO/CdO and ZnO/ZnCdO nanowires grown by MBE on Si (111) substrate. For these experiments, two excitation wavelengths of 514.5 nm and 325 nm were used. Both the non-resonance and the resonance Raman spectra of the ZnO/ZnCdO and ZnO CdO MQW heterostructures reveal a redshift of the Raman peaks relative to bulk ZnO. Moreover, for the ZnO/CdO sample, a significant broadening of the  $\text{A}_1^{\text{LO}}$  line occurs, compared to pure ZnO. Both effects, the redshift and the broadening of ZnO related phonon modes, revealed the type of tensile strain occurring in the analyzed samples. The XRD signals having their source in the ZnO and MQW buffers are also significantly broadened. This effect was attributed to micro-strains in nanowires. Thus, based on the  $\mu$ -Raman and HR-XRD measurements, the value of micro-deformations for the tested samples was estimated, and the obtained results were consistent with each other. A detailed description and interpretation can be found in [D8]

The planar structures and nanocolumns grown on silicon with various buffer layers and in various growth conditions, were used later as p-n junction structures to perform additional electric measurements (I-V, C-V, DLTS). Electric measurements were performed in Wrocław University of Science and Technology, and the results are presented in works [D9-D13].

I also participated in the study of cubic CdO /MgO superlattices on *r*-plane sapphire grown using the MBE method [D14].

[D1] E. Przedziecka, A. Wierzbička, A. Reszka, K. Gościński, A. Droba, R. Jakięła, D.Dobosz, T. A. Krajewski, K. Kopalko, J. M. Sajkowski, M. Stachowicz, **M. A. Pietrzyk**, A. Kozanecki, *Characteristics of ZnO:As/GaN heterojunction diodes obtained by PA-MBE*, Journal of Physics D: Applied Physics 46, 035101 (2013),

[D2] E. Przedziecka, K. Goscinski, M. Stachowicz, D. Dobosz, E. Zielony, J.M. Sajkowski, **M.A. Pietrzyk**, E. Placzek-Popko, A. Kozanecki, *Spectrum selective UV detectors from an p-ZnO:As/n-GaN diodes grown by Molecular Beam Epitaxy*, Sensor. Actuator. A – Phys. 195, 27 (2013)

[D3] E. Przedziecka, A. Wierzbička, P. Dłuzewski, M. Stachowicz, R. Jakięła, K. Goscinski, **M. A. Pietrzyk**, K. Kopalko, and A. Kozanecki, *Dual-acceptor doped p-ZnO:(As,Sb)/n-GaN heterojunctions grown by PA-MBE as a spectrum selective ultraviolet photodetector*, Phys. Status Solidi A 211, 2072-2077 (2014)

[D4] E. Przedziecka, W. Lisowski, R. Jakiela, J. W. Sobczak, A. Jablonski, **M. A. Pietrzyk**, A. Kozanecki, *Arsenic chemical state in MBE grown epitaxial ZnO layers – doped with As, N and Sb*, J. Alloys Compd. 687, 937-942 (2016)

[D5] M. Stachowicz, J.M. Sajkowski, S. Kryvyi, A. Pieniazek, A. Reszka, A. Wierzbicka, **M.A. Pietrzyk**, E. Przedziecka, D. Jarosz, K. Gwozdz, E. Placzek-Popko, E. Alves, S. Magalhaes, A. Kozanecki, *Study of structural and optical properties of MBE grown nonpolar (10-10) ZnO/ZnMgO photonic structures*, Opt. Mater. 100, 109709 (2020),

[D6] M. Stachowicz, J.M. Sajkowski, A. Wierzbicka, E. Przedziecka, **M.A. Pietrzyk**, E. Dynowska, S. Magalhaes, E. Alves, A. Kozanecki, *Nonpolar short-period ZnO/MgO superlattices: Radiative excitons analysis*, J. Lumin. 238, 118288 (2021)

[D7] A. Wierzbicka, **M.A. Pietrzyk**, A. Reszka, J. Dyczewski, J.M. Sajkowski, A. Kozanecki, *Strain distribution in  $Mg_xZn_{1-x}O$  layers with various content of Mg grown on a-plane sapphire by plasma-assisted molecular beam epitaxy*, Appl. Surf. Sci. 404, 28-33 (2017)

[D8] E. Zielony, A. Wierzbicka, R. Szymon, **M.A. Pietrzyk**, E. Placzek-Popko, *Investigation of micro-strain in ZnO/(Cd,Zn)O multiple quantum well nanowires grown on Si by MBE*, Appl. Surf. Sci. 538, 148061 (2021)

[D9] E. Placzek-Popko, K. M. Paradowska, **M. A. Pietrzyk**, Z. Gumienny, P. Biegański A. Kozanecki, *Deep traps and photo-electric properties of p-Si/MgO/n-Zn<sub>1-x</sub>Mg<sub>x</sub>O heterojunction*, J. Appl. Phys. 118, 074501 (2015)

[D10] K.M. Paradowska, E. Placzek-Popko, K. Gwóźdź, **M.A. Pietrzyk**, A. Kozanecki, *Current transport and deep levels in p-Si/n-Zn<sub>0.9</sub>Mg<sub>0.1</sub>O/n-ZnO heterojunction*, J. Alloys Compd. 691, 946-951 (2017)

[D11] **M.A. Pietrzyk**, E. Zielony, M. Stachowicz, A. Reszka, E. Placzek-Popko, A. Wierzbicka, E. Przedziecka, A. Droba, A. Kozanecki, *Electro-optical characterization of ZnO/ZnMgO structure grown on p-type Si (111) by PA-MBE method*, J. Alloys Compd. 587, 724-728 (2014)

[D12] E. Zielony, **M.A. Pietrzyk**, *Diode characteristics of ZnO/ZnMgO nanowire p-n junctions grown on Si by molecular beam epitaxy*, Mater. Sci. Eng. B-Adv. 268, 115148 (2021)

[D13] E. Placzek-Popko, K. M. Paradowska, **M. A. Pietrzyk**, A. Kozanecki, *Carrier transport mechanisms in the ZnO based heterojunctions grown by MBE*, Opto-Elektron. Rev. 25, 181-187 (2017)

[D14] E. Przedziecka, A. Wierzbicka, P. Dłużewski, I. Sankowska, P. Sybilski, K. Morawiec, **M. A. Pietrzyk**, A. Kozanecki, *Short-Period CdO/MgO Superlattices as Cubic CdMgO Quasi-Alloys*, Cryst. Growth Des. 20, 5466–5472 (2020)

### **5.3. Information on presentations at national or international scientific or artistic conferences, detailing the invited lectures and plenary lectures.**

### Invited oral presentations given by co-authors:

J1. E. Guzewicz, D. Snigurenko, T.A. Krajewski, E. Przeździecka, D. Jarosz, **M. A. Pietrzyk**, B.S. Witkowski,  
*p-type ZnO and nanostructured ZnO-based homojunction grown at low temperature*,  
Energy Materials Nanotechnology Prague Meeting 2016 (EMN 2016), June 21-24, 2016,  
Prague, Czech Republic.

### Other oral presentations given personally at domestic and international conferences

O1. **M. A. Pietrzyk**, M. Stachowicz, A. Reszka, A. Wierzbicka, A. Kozanecki,  
*Self-organized ZnMgO nanocolumns with ZnO/ZnMgO quantum wells grown on different substrates by MBE technique*,  
11<sup>th</sup> International conference on Advanced Nanomaterials, Aveiro, Portugalia lipiec 2018

O2. **M.A. Pietrzyk**, M. Stachowicz, A. Reszka, A. Wierzbicka, A. Kozanecki,  
*Properties of ZnO/ZnMgO nanocolumns obtained on Si and polar/nonpolar Al<sub>2</sub>O<sub>3</sub> substrates by MBE technique*,  
International Union of Materials Research Societies- The 15th International Conference on  
Advanced Materials, 27 sierpnia- 1 września 2017, Kioto, Japonia

O3. **M.A. Pietrzyk**, M. Stachowicz, A. Wierzbicka, A. Kozanecki,  
*Optical investigations of ZnO/ZnMgO quantum wells in self-assembled ZnMgO nanocolumns grown on different substrates by MBE technique*,  
International Union of Materials Research Societies- International Conference on Advanced  
Materials, 4-8 lipca 2016, Singapur

O4. **M.A. Pietrzyk**, M. Stachowicz, R. Minikayev, A. Kozanecki,  
*Optical and structural properties of ZnO/ZnMgO nanostructures grown on r-plane Al<sub>2</sub>O<sub>3</sub> and Si (111) substrates by MBE*,  
14th International Union of Materials Research Societies- International Conference on  
Advanced Materials, 25-29 Październik 2015 Jeju, Korea

O5. **M. A. Pietrzyk**, M. Stachowicz, D. Jarosz, E. Przeździecka, A. Reszka, J. M. Sajkowski,  
A. Kozanecki;  
*Self-assembled ZnMgO nanocolumns grown on Si (111) with ZnO quantum wells – optical and structural properties*;  
E-MRS 2014 Fall Meeting Warsaw

O6. **M.A Pietrzyk**, M. Stachowicz, D. Jarosz, E. Przeździecka, A. Reszka, A. Kozanecki,  
*ZnO quantum wells in ZnMgO nanocolumns grown on Si (111) by MBE-optical and structural properties*,  
BIT's 3rd Annual World Congress of Advanced materials (2014) Chongqing, Chiny.

O7. **M. A. Pietrzyk**, A. Reszka, M. Stachowicz, A. Droba, A. Wierzbicka, J. M. Sajkowski,  
E. Przeździecka, A. Kozanecki;  
*Optical and structural properties of ZnO quantum wells in ZnMgO nanocolumns grown on Si (111) by MBE*;  
E-MRS 2013 Fall Meeting Warsaw

O8. **M.A. Pietrzyk**, A. Reszka, M. Stachowicz, A. Droba, A. Wierzbicka, E. Przeździecka, A. Kozanecki,  
*PA-MBE grown ZnMgO/ZnO/ZnMgO heterostructures on p-type Si (111) – optical properties*,  
BIT's 2nd Annual World Congress of Advanced materials (2013) Suzhou, Chiny

Moreover, I was co-author of 16 oral presentations (given by my co-workers), as well as an author or co-author of about 80 poster presentations at international conferences.

### **Seminar presentations**

I have given 4 seminar presentations related to the subject of habilitation:

S1. **M. A. Pietrzyk**, *Studnie kwantowe ZnO w nanosłupkach ZnMgO wzrastanych na wybranych podłożach*, Instytut Fizyki – Centrum Naukowo-Dydaktyczne, Politechnika Śląska, 23 maja 2018

S2. **M. A. Pietrzyk**, *Studnie kwantowe ZnO w nanosłupkach ZnMgO wzrastanych na podłożach szafirowych oraz na krzemie*, Seminarium z Fizyki Ciała Stałego, Wydział Fizyki UW, 17 marca 2017

S3. **M. A. Pietrzyk**, *Studnie kwantowe ZnO w nanosłupkach ZnMgO otrzymywane metodą MBE na wybranych podłożach*, Seminarium oddziałowe ON 4, 2016

S4. **M. A. Pietrzyk**, *Badania właściwości optycznych i strukturalnych pojedynczych i wielokrotnych studni kwantowych w nanosłupkach ZnMgO wzrastanych na podłożu Si (111) metodą MBE*, Seminarium oddziałowe ON 4, 2013

### **5.4 Information on participation in the organizational and scientific committees of national or international conferences, including the function performed.**

I was a member of the organizing committee of conference „10<sup>th</sup> International Workshop on Zinc Oxide and Other Oxide Semiconductors”, held in September 2018 in Warsaw.

### **5.5 Information on participation in the work of research teams implementing projects financed through domestic or foreign competitions/grants, with a division into completed and ongoing projects, and including information on the function performed within the team's work.**

From 2014 to 2018 I was the Principal Investigator the NCN founded SONATA project No. 2013/09/D/ST5/03881 "ZnO quantum wells in ZnMgO nanocolumns grown on selected substrates with MBE technique"

From 2007 to 2013 I participated in NanoBiom project No. POIG.01.01.02-00-008/08 (NANOBIOM) „Quantum semiconductor nanostructures for applications in biology and medicine – development and commercialisation of new generation devices for molecular diagnostics on the basis of new Polish semiconductor devices”, in the framework of the Operational Programme Innovative Economy 2007 – 2013

## **5.6 Information on internships in scientific or artistic institutions, including foreign ones, including the place, date, duration, and nature of the internship.**

Before PhD:

1. Germany (Hamburg) DESY/ HASYLAB synchrotron laboratory, research visit, 2005-2010, 6 weeks/year, 2011-2012, 1 week/year.

Receiving person: prof. Robert L. Johnson

2. Sweden (Lund) MAX-lab synchrotron laboratory, 2005-2010, 2 weeks/year.

Receiving person: prof. Janusz Kanski

3. Belgium (Namur), Laboratory for Electron Spectroscopy, University Notre-Dame de la Paix in Namur, research visits, 2005-2010, 1-2 weeks/year

Receiving person: prof. Jacques Ghijsen.

After PhD:

1. Germany (Hamburg) DESY/ HASYLAB synchrotron laboratory, research visit, 2011-2012, 2 weeks/year,

Receiving person: prof. Robert L. Johnson

2. Belgium (Namur), Laboratory for Electron Spectroscopy, University Notre-Dame de la Paix in Namur, research visits, 2011, 2 weeks/year

Receiving person: prof. Jacques Ghijsen.

## **5.7 Information on peer-reviewed scientific or artistic papers, in particular those published in international journals.**

I was a reviewer for scientific journals such as:

ACS Applied Nano Materials - 1 review,

Journal of Alloys and Compounds - 5 reviews,

Acta Phys. Pol. A - 2 reviews,

Applied Physics A-1 review,

Optics Communications- 1 review,

IEEE Transactions on Industrial Electronics - 1 review

Journal of Crystal Growth - 1 review

Sensors and Actuators B- Chemical - 1 review

Materials – 1 review

## **5.8 Obtained industrial property rights, including obtained patents, national or international**

Patents:

**P. 416263** *Złącza elektryczne na bazie tlenku cynku oraz sposób wykonania tego złącza*

authors: Elżbieta Guzewicz, **Mieczysław Pietrzyk**, Ewa Przeździecka, Dymitr Snigurenko

**P. 423624** *Sposób wytwarzania struktur z trójskładnikowymi warstwami  $Zn_{1-x}Mg_xO$*

authors: Dawid Jarosz, Henryk Teisseyre, Marcin Stachowicz, **Mieczysław Pietrzyk**, Ewa Przeździecka, Jacek Sajkowski, Adrian Kozanecki

Patent applications:

**P.416262** *Sposób wytwarzania nanokolumn na bazie ZnO oraz struktura nanokolumnowa wytworzona tym sposobem*

author: **Mieczysław Pietrzyk**

## **5.9 Information on expert opinions or other studies commissioned by public institutions or entrepreneurs.**

Review of the SONATA grant application for the NCN National Science Center

## **6. Information about the achievements in teaching, organization and popularizing science or art.**

### **Supervision:**

Auxiliary supervisor of the doctoral dissertation Abinasha Adhikari.

### **Tutor of student internships:**

2018 Maciej Daukso - Politechnika Warszawska

2016 Wojciech Zduńczyk – Politechnika Warszawska

2013 Stanisław Sołtan – Uniwersytet Warszawski

## **7. In addition to the issues listed in point 1-6, the applicant may provide other information, important from his point of view, regarding his professional career**

### **Prizes and awards**

**2015:** Award for the best poster at the 14th International Union of Materials Research Societies-International Conference on Advanced Materials (IUMRS-ICAM 2015), Jeju, Korea

**2009:** Mazovia Scholarship for PhD students - a part of "Regional Innovation Strategy and Transfer of Knowledge" project, partially supported by the European Social Fund within Integrated Regional Development Programme